9

Review Article

Xin Long, Xiongbang Wei, Yuhong Qiu, Yaochen Song, Linnan Bi, Pengkai Tang, Xingbin Yan*, Sizhe Wang*, and Jiaxuan Liao*

TiO₂ aerogel composite high-efficiency photocatalysts for environmental treatment and hydrogen energy production

https://doi.org/10.1515/ntrev-2022-0490 received May 7, 2022; accepted September 14, 2022

Abstract: Photocatalysis is a new type of renewable energy technology used in environmental treatment and hydrogen energy production. In this regard, a new class of photocatalysts, TiO₂ aerogels, are attractive for having the chemical characteristics of TiO₂ nanomaterials such as high catalytic activity, good stability, non-toxic, and non-polluting, and the structural characteristics of aerogels such as large specific surface area, high porosity, the 3-dimensional interconnected network structure composed of relatively uniform nanoparticles, and high light transmittance. Here we review the recent progress in TiO₂ aerogels for photocatalysis, focusing on preparation techniques, the crystalline phases' influence on photocatalytic properties, the modification of

photocatalytic properties, and the analysis and discussion of future development. In particular, we first summarize various preparation techniques, including sol-gel method, nanoparticles self-assembly synthesis, and high-temperature aerosol technique, then detail the structure and composition of TiO₂ crystalline phases that affect the photocatalytic properties. Subsequently, we discuss strategies to further enhance the photocatalytic properties of TiO2 aerogels by the composite of SiO₂ aerogel semiconductors, the doping of metal dopants, and the doping or composite of non-metallic substances, and elaborate the modification mechanism and the modification effect achieved. Finally, combined with the research status of TiO₂ aerogels and the development experience of other aerogels, we conduct a reasonable analysis and discussion on their further research directions and industrialization roads.

Keywords: TiO₂ aerogels, composite, photocatalysis, environmental treatment, hydrogen energy production

* Corresponding author: Jiaxuan Liao, The Yangtze Delta Region

China, Chengdu, 611731, China

1 Introduction

Environmental pollution and energy shortage have become two major problems hindering the progress of human society [1,2]. With the deepening of understanding, countries all over the world are striving to control environmental pollution and develop new energy sources, and the exploitation of solar energy is in full swing [3–5]. Since Fujishima and Honda [6] discovered the photocatalytic decomposition of water on the N-type semiconductor TiO2 in 1972 and opened up a new field of photocatalysis, the technology has received widespread attention. According to the current application requirements, photocatalysis can be divided into environmental photocatalysis and energy photocatalysis [7,8]. The environmental photocatalysis refers to the decomposition of environmental pollutants, viruses, and bacteria through chemical reactions driven by sunlight to achieve the purpose of environmental protection [9,10],

^{*} Corresponding author: Xingbin Yan, School of Materials Science and Engineering, Sun Yat-Sen University, Guangzhou, 510275, China, e-mail: yanxb3@mail.sysu.edu.cn

^{*} Corresponding author: Sizhe Wang, The Yangtze Delta Region Institute (Quzhou), University of Electronic Science and Technology of China, Quzhou, Zhejiang, 324003, China; Shaanxi Key Laboratory of Green Preparation and Functionalization for Inorganic Materials, Shaanxi University of Science & Technology, Xi'an, 710021, China, e-mail: kevinwang@sust.edu.cn

Institute (Quzhou), University of Electronic Science and Technology of China, Quzhou, Zhejiang, 324003, China; School of Materials and Energy, University of Electronic Science and Technology of China, Chengdu, 611731, China, e-mail: jxliao@uestc.edu.cn

Xin Long, Yuhong Qiu, Yaochen Song, Linnan Bi, Pengkai Tang: The Yangtze Delta Region Institute (Quzhou), University of Electronic Science and Technology of China, Quzhou, Zhejiang, 324003, China; School of Materials and Energy, University of Electronic Science and Technology of China, Chengdu, 611731, China

Xiongbang Wei: The Yangtze Delta Region Institute (Quzhou), University of Electronic Science and Technology of China, Quzhou, Zhejiang, 324003, China; School of Optoelectronic Science and Engineering, University of Electronic Science and Technology of

and the energy photocatalysis refers to the conversion of lowenergy-density solar energy into high-energy-density hydrogen energy to realize the production of new energy [11]. From the perspective of cost, safety, and sustainability of technological development, photocatalytic technique is obviously very promising.

At the end of the twentieth century, the advent of TiO₂ aerogels successfully promoted the further development of TiO₂ nanomaterials in the field of photocatalysis [12]. Nowadays, three relatively mature technologies for preparing TiO₂ aerogels have been formed: 1) the most commonly used sol-gel method for the preparation of TiO₂ aerogels with amorphous structure [13]; 2) the nanoparticles self-assembly synthesis for the preparation of TiO₂ aerogels with controllable crystalline phase composition [14]; 3) the high-temperature aerosol engineering technique for the preparation of highly crystalline and highly pure structured TiO₂ aerogels [15]. These methods can construct a highly porous 3-dimensional TiO₂ aerogels' framework structure. It is precisely because of the aerogels' framework structure that the photocatalytic properties of TiO2 aerogels are far superior to other types of TiO₂ nanomaterials. Their high specific surface area can provide a larger reaction area, resulting in more reaction occasions [16], high porosity is beneficial to ensure the adsorption and accommodation of reactants to form a synergistic effect of reaction and adsorption [17], 3-dimensional interconnected network structure is conducive to the mass transfer process [18], and translucent structure can be simultaneously excited by light on the inner and outer surfaces to form more active electron-hole pairs, thereby generating more reactive centers [19], and these structural advantages all help to accelerate the progress of the photocatalytic reaction. In addition, the TiO₂ aerogels in block form are very easy to realize the process of recycle and reuse, which effectively avoids the drawbacks of the secondary pollution caused by partial TiO₂ nanomaterials such as powders and fibers that cannot be recycled, it is also one of the structural advantages of aerogels [20].

But even so, TiO2 aerogels have some limitations in structures and photocatalytic properties. In terms of structures, the adsorption properties of TiO2 aerogels are generally weak, and it is difficult to achieve the synergistic effect of photocatalysis and adsorption at low concentrations of reactants [21], and the poor mechanical properties of pulverization and fragility also limit their practical application [22]. Moreover, the most important characteristic of high-efficiency photocatalysts is the effectiveness of solar energy conversion, which depends on four factors: light absorption, charge separation, charge migration, and charge recombination [23]. Considering these factors, the

shortcoming of TiO₂ aerogels in terms of photocatalytic properties is that the relatively large bandgap energy of 3.0-3.2 eV needs UV-excitation, which comprises only 5% of solar radiation, and the short lifetime of the active electron-hole pairs obtained by light excitation can also reduce the quantum efficiency of the photocatalytic reaction.

In order to overcome the intrinsic limitations of TiO₂ aerogels, modification methods of doping and compositing have been widely used [24,25]. According to different modification mechanisms, we reasonably divide the substances used for modification into three categories: SiO₂ aerogels, metal dopants, and non-metallic substances. Compared with TiO₂ aerogels, SiO₂ aerogels have more excellent structural characteristics of aerogels [26,27]. Therefore, TiO₂ aerogels can rely on the structure of SiO₂ aerogels to exert better photocatalytic properties, and the formation of two aerogels' composite structure is also conducive in prolonging the lifetime of active electron-hole pairs and controlling the stability of the crystallized TiO₂ to a certain extent [28]. The doping of metal dopants mainly reduces the bandgap width of TiO₂ aerogels to improve the utilization of sunlight, accelerates the formation of electron-hole pairs, and prolongs their lifetime, and promotes the formation of the crystallized TiO₂ to speed up the quantum efficiency of the photocatalysis [29]. The modification mechanism of non-metallic substances is generally more complicated. Some of them can produce a modification effect similar to that of metal dopants [30], and others can enhance the photocatalytic properties of TiO₂ aerogels through intrinsic properties [31]. For instance, the TiO₂–C composite aerogel realizes the electrochemical adsorption process enhanced by photocatalysis [32], the TiO₂-sodium alginate composite aerogel realizes an underwater oleophobic function [31], and the TiO₂-graphene composite aerogel realizes the synergistic effect of photocatalysis and high-efficiency adsorption [33].

Up to now, a total of more than 100 research have conducted relatively systematic studies on TiO₂ aerogels, partially solving the problems in the preparation and properties improvement. But meanwhile, many challenges that urgently need to be broken have also been left behind. For instance, most of the reported studies focus on the improvement of the photocatalytic properties of TiO₂ aerogels, and there are few reports specifically aimed at the improvement of mechanical properties. Although a variety of techniques have been developed to prepare TiO2 aerogels with different structural characteristics, the industrialization process of TiO₂ aerogels is still very slow. These all have left us a lot of space for thinking and studying.

On the basis of the above contents, we first introduce three techniques that can prepare TiO₂ aerogels with

Figure 1: General overview of the preparation, modification, and application of TiO₂ aerogel composites. Modified with permission from ref. [34]. Copyright 2019, American Chemical Society.

different structures and properties, and systematically analyze the influence of TiO₂ crystalline phases on photocatalytic properties. Subsequently, we summarize the modification methods of TiO₂ aerogels for environmental treatment and hydrogen energy production, and elaborate the modification mechanism and the modification effect achieved. Finally, combined with the research status of TiO₂ aerogels and the development experience of other aerogels, we put forward our own insights on the future development directions and industrialization roads of TiO2 aerogels (Figure 1).

2 Preparation techniques

2.1 Sol-gel method

DE GRUYTER

Among the relevant research reports currently available, most of them have used the sol-gel method to prepare TiO₂ aerogels. The sol–gel method has obvious advantages from others techniques due to the mixing of reaction components at the atomic scale, simplicity of operation, and low cost [25,35]. The process includes two reaction steps: hydrolysis and polycondensation, as shown in Figure 2(a). The Ti-containing precursor first undergoes a hydrolysis reaction to form primary particles-Ti(OH)₄, and then the primary particles undergo dehydration and condensation reactions to form the basic components of the TiO2 aerogels' skeleton network-secondary particles [36]. Subsequently, infinite number of secondary particles are randomly cross-linked

in 3-dimensional space to initially build the skeleton structure of TiO₂ wet gel. It is worth mentioning that the above reaction steps have no obvious boundaries in the sol-gel reaction process, and they almost exist and proceed simultaneously [16]. After the sol-gel reaction, an aging process is usually needed to strengthen the neck areas between the secondary particles to improve the mechanical properties of the resulting TiO_2 wet gel (Figure 2(b)) [37].

Finally, what needs to be done is the drying process of the TiO₂ wet gel. Generally, the liquid surface curvature formed when the solvents in the wet gel volatilize is in the same order of magnitude as the pore size of the wet gel, thereby the surface tension formed between the solidliquid interface can easily cause the shrinkage and structural collapse of the wet gel, which makes the drying of the wet gel require some special drying methods [35,38]. For the TiO₂ wet gel, supercritical drying and ambient pressure drying are mainly used. The supercritical drying refers to the use of supercritical fluid extraction to eliminate the surface tension of the solvents to complete the drying process and transform wet gel to aerogel while maintaining the structure of the gel skeleton [39], which requires not only expensive and complex supercritical drying equipment, but also usually high-temperature and high-pressure operating conditions. Therefore, the technique can only be applied on a laboratory scale and is difficult to be extended to industrial production. Since then, in order to avoid the complicated and harsh drying environment and for the sake of safety, the ambient pressure drying for the TiO2 wet gel is proposed, which mainly includes the following steps: 1) the surface modification, 2) the low surface tension solvent replacement,

4 — Xin Long et al. DE GRUYTER

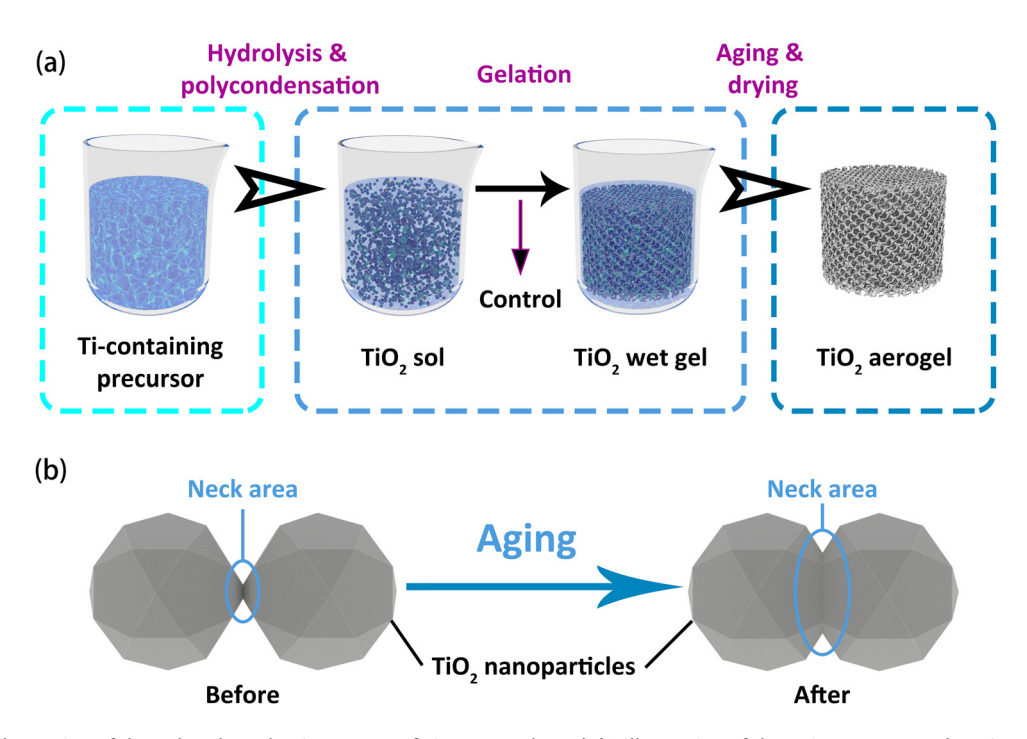


Figure 2: (a) Illustration of the sol-gel synthesis process of TiO_2 aerogels and (b) illustration of the aging process enhancing the neck areas of secondary particles.

and (3) the drying under ambient pressure [40]. Thereinto, siloxane-based surfactants are the most widely used in the modification of the TiO_2 wet gel in step (1) because they can react incompletely reacted -OH to $-OSi(C_nH_{2n+1})_3$, which not only avoids the structural collapse of the TiO_2 wet gel caused by the continuous condensation reaction of -OH during the drying process, but also improves its hydrophobic properties [41,42]. N-hexane is the most frequently used replacement solvent for the TiO_2 wet gel in step (2) due to its low surface tension of 17.89 dyne/cm [43]. Although the quality of TiO_2 aerogels obtained by the ambient pressure drying is slightly inferior to that obtained by the supercritical drying, from the perspective of large-scale production of TiO_2 aerogels, the ambient pressure drying is obviously a better choice.

2.2 Nanoparticles self-assembly synthesis

The photocatalytic properties of TiO_2 aerogels can only be displayed in the crystalline state, while the TiO_2 aerogels prepared by the sol–gel method are usually amorphous and need to be crystallized at a high temperature before they can be used [37]. However, high-temperature treatment usually leads to the destruction of the TiO_2 aerogels' structure, and the low-porosity crystalline aggregates formed during the process often further weaken the

structural characteristics of the aerogel [44]. Undoubtedly, for the TiO₂ aerogels prepared by the sol–gel method, it is difficult to find a balance between the structural characteristics of aerogels and the formation of crystalline phases. Based on this problem, the second method of preparing TiO₂ aerogels-nanoparticles self-assembly synthesis is proposed [14], which mainly completes the oriental attachment process in the 3-dimensional direction through the surface polymerization of specially treated crystalline TiO₂ nanoparticles, thereby constructing a highly porous TiO₂ wet gel's skeleton network, and then the desired TiO₂ aerogels are obtained by the supercritical drying or the ambient pressure drying (Figure 3(a)).

Generally, the nanoparticles self-assembly synthetic ${\rm TiO_2}$ aerogels have the structural characteristics of macroporous aerogels, a super-high proportion of crystalline phase composition, and multiple crystalline phases that can exist simultaneously, which successfully overcomes the limitations of the sol–gel preparation of ${\rm TiO_2}$ aerogels [18]. However, it should be emphasized that the main problem of the self-assembly of nanoparticles to synthesize ${\rm TiO_2}$ aerogels is the short-range order of the assembly of ${\rm TiO_2}$ nanoparticles. Generally, the spontaneous assembly size of crystalline ${\rm TiO_2}$ nanoparticles is less than 1 $\mu {\rm m}$, and the assembly direction is mostly 1-dimensional, so it is difficult to obtain nano-structured 3-dimensional porous materials. The core idea to solve this problem is to modify

Figure 3: (a) Assembly of TiO₂ nanoparticles using either trizma-functionalized nanoparticles or non-functionalized nanoparticles; (b) photographs of the self-assembled TiO₂ aerogel and the trizma-functionalized TiO₂ nanoparticles; and (c) detailed HRTEM image of a part of the self-assembled TiO₂ aerogel, showing the linear subunits and the misoriented junctions. (b) and (c) Modified with permission from ref. [14]. Copyright 2011, Royal Society of Chemistry.

the crystalline TiO₂ nanoparticles to achieve an anisotropic polymerization, thereby constructing a 3-dimensional aerogels' skeleton network structure. Thereinto, the polymerization process is maintained by directional adsorption, in which adjacent nanoparticles coalesce spontaneously in such a way to share a common crystallographic orientation, and only in this case the size of the self-assembled product can be extended to the cm range (Figure 3(b)). In the reports on the synthesis of TiO2 aerogels by the self-assembly of nanoparticles, trizma is the most widely used for the surface functional modification of crystalline TiO2 nanoparticles [14]. These treated nanoparticles can self-assemble into macroporous TiO₂ aerogels with irregular block shapes, which is the result of the directional attachment process experienced by the nanoparticles after the trizma stabilizer is selectively removed from the {001} crystalline plane, as exhibited in Figure 3(c).

DE GRUYTER

2.3 High-temperature aerosol technique

Different from the two techniques mentioned above, the high temperature aerosol technique uses the idea of gasphase synthesis to prepare TiO₂ aerogels. The method first forms TiO₂ nanoparticles by evaporating and decomposing the Ti-containing aerosol obtained from the Ti-containing precursor under the accompaniment of selected reaction gases, then adjusts the conditions in the reaction device through a computer program so that the nanoparticles are assembled in 3-dimensional directions under control, and TiO₂ aerogels with a highly porous structure are successfully prepared, the detailed process is shown in Figure 4 [15]. During this process, the structural characteristics of the obtained TiO₂ aerogels such as particle size, porosity, specific surface area, crystallinity, composition of crystalline phases, etc., are determined by the interaction of preset temperature gradient, precursor concentration, the amount of reactant gases, residence time, etc. To understand the relevance of these conditions, the preparation of TiO₂ aerogels with different structures and properties can be realized.

In addition, the nanoparticles in the TiO2 aerogels prepared by the high-temperature aerosol technique are highly pure, highly crystalline, and their surface does not contain any additives. But the two methods mentioned above belong to the liquid phase synthesis, a variety of solvents and chemical additives used to adjust the structure of the wet gel are more or less used, which makes the obtained TiO₂ aerogels impossible to be highly pure [18,45]. It can be concluded that the high temperature aerosol technique has some significant advantages in the preparation of highly crystalline and highly pure structured TiO₂ aerogels. However, the controllability of the technique is far less than the previous two methods, and it is difficult to understand the influence of the diversity of influencing factors and the complexity of these related factors on the structures and properties of the prepared TiO2 aerogels. Thus, the sol-gel method and the nanoparticles self-assembly synthesis belonging to liquid-phase synthesis and the high temperature aerosol technique belonging to gas-phase synthesis can be complementary to a certain extent in the specific aspects of preparing TiO₂ aerogels. For instance, the use of sol-gel method and high-temperature aerosol engineering can make the amorphous TiO2 and crystalline TiO2 distributed in different regions of TiO₂ aerogels. In the inner region, the

6 — Xin Long et al. DE GRUYTER

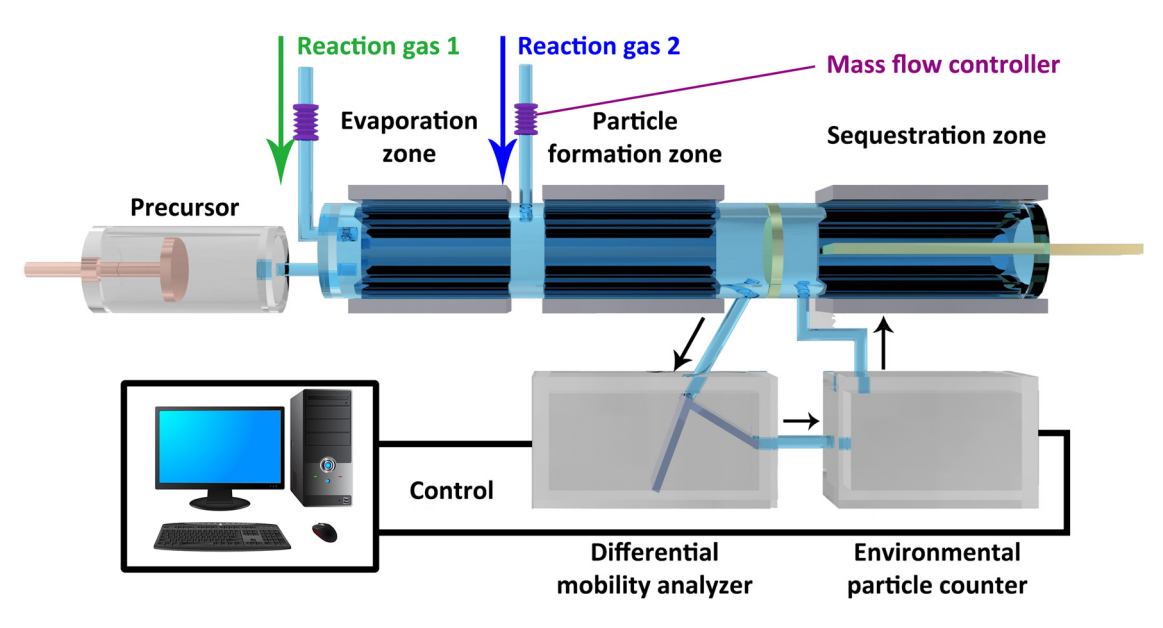


Figure 4: The flow chart of the device for synthesizing TiO₂ aerogels by the high-temperature aerosol engineering.

sol–gel method forms an amorphous TiO_2 aerogel skeleton structure, maintaining the remarkable aerogel structural properties. In the outer region, high-temperature aerosols form highly crystalline TiO_2 aerogels to perform photocatalytic reactions. In this way, the inner regions where light cannot penetrate are composed of amorphous TiO_2 aerogels to provide structural support, and the regions where light can shine are composed of crystalline TiO_2 aerogels for photocatalytic reactions, and the photocatalytic properties of the resulting TiO_2 aerogels can be effectively enhanced [46]. It may also be one of the directions to be explored in the preparation of TiO_2 aerogels in the future.

3 Influence of crystalline phases on the photocatalytic properties of TiO₂ aerogels

The crystalline phases of TiO_2 aerogels greatly affect the progress rate of the photocatalytic reaction. Among the different crystalline phases, it is generally accepted that anatase TiO_2 has the strongest catalytic activity, followed by rutile TiO_2 , and brookite TiO_2 and amorphous TiO_2 are the weakest [44]. In terms of crystalline structures, both anatase TiO_2 and rutile TiO_2 have a tetragonal crystalline structure formed by TiO_6 octahedral chains, that is, every Ti atom in the unit cell is surrounded by six oxygen atoms, but their assembly mode of the octahedral chain and distortion method of the octahedron are completely

different [2,47]. In anatase TiO₂, the orthogonality of TiO₆ octahedrons is higher than that of the symmetry, and each octahedron is connected to eight adjacent octahedrons. Thereinto, every four unit cells share an edge, and every four unit cells share an angle (Figure 5(a)). And in rutile TiO₂, TiO₆ octahedrons exhibit irregular orthogonal distortions, and each octahedron is connected to 10 adjacent octahedrons. Thereinto, every two octahedrons share an edge oxygen atom pairs and every eight octahedrons share corner oxygen atoms (Figure 5(b)). In addition, the Ti-O bond length in rutile TiO₂ is longer than that of anatase TiO₂, while the Ti-Ti bond length is shorter [48]. It is precisely because of the abovementioned difference in the crystalline structures wherein the electronic band structure and mass density of anatase TiO₂ and rutile TiO₂ are completely different, which causes their photocatalytic intrinsic properties to be completely different [49].

In terms of photocatalytic properties, the content and ratio of anatase ${\rm TiO_2}$ and rutile ${\rm TiO_2}$ are one of the main factors affecting the properties of ${\rm TiO_2}$ aerogels [50]. The valence band positions of these 2 crystalline phases are the same, and the formed photo-generated holes have the same oxidation properties. However, the bandgap of anatase ${\rm TiO_2}$ is 3.2 eV, which is higher than the 3.0 eV of rutile ${\rm TiO_2}$, indicating that the conduction band potential of anatase ${\rm TiO_2}$ is more negative, and the photogenerated electrons formed have stronger reducing ability. Also, the lower bandgap of rutile ${\rm TiO_2}$ easily causes the recombination of photoexcited electron–hole pairs, resulting in a decrease in catalytic activity, so the formation of anatase ${\rm TiO_2}$ is very beneficial to improve the photocatalytic

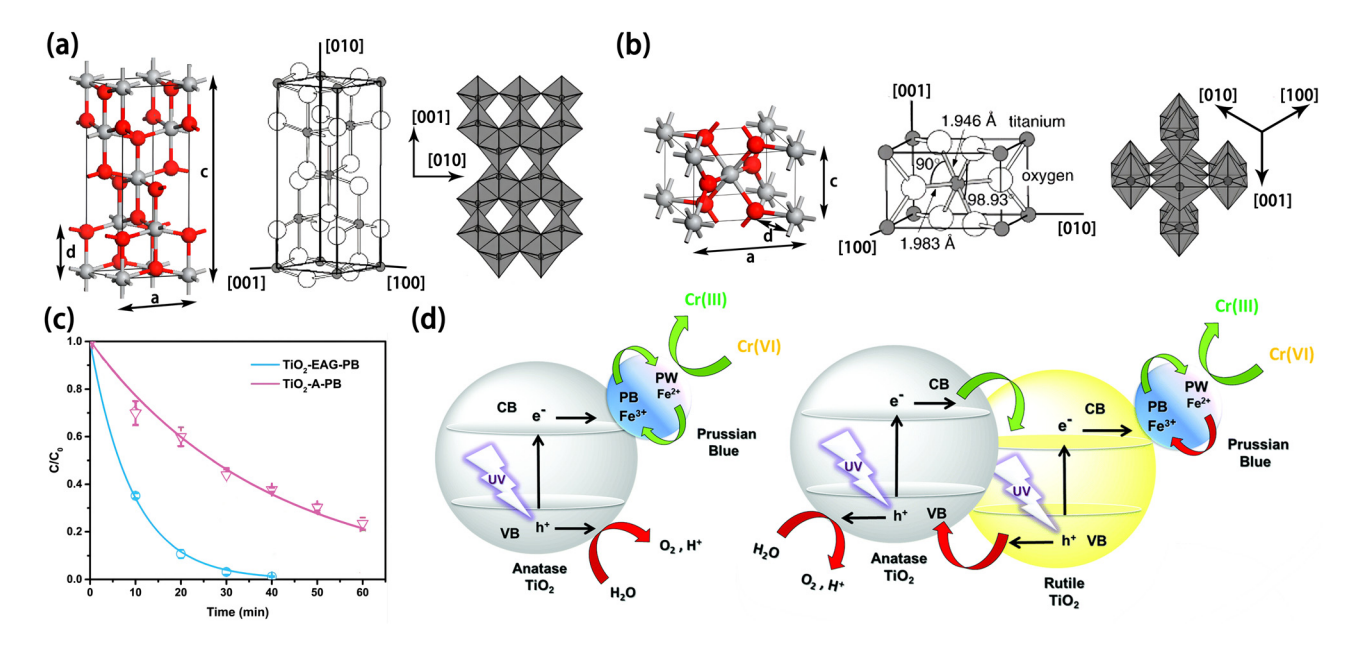


Figure 5: (a) Tetragonal structures and unit cell structures of anatase TiO_2 described by using two cell edge parameters – a and c, and one internal parameter – d; (b) tetragonal structures and unit cell structures of rutile TiO_2 described by using two cell edge parameters – a and c, and one internal parameter – d; (c) kinetic curves of the photocatalytic degradation of Cr^{6+} by the TiO_2 -EAG-PB (the Prussian blue modified TiO_2 aerogel containing appropriate ratio of anatase TiO_2 and rutile TiO_2 and the TiO_2 -A-PB (the Prussian blue modified TiO_2 aerogel containing only anatase TiO_2); and (d) illustration of the mechanism of the mixed crystal effect of anatase TiO_2 and rutile TiO_2 . (a) and (b) Modified with permission from ref. [2]. Copyright 2019, Springer. (c) and (d) Modified with permission from ref. [50]. Copyright 2021, Royal Society of Chemistry.

properties of TiO₂ aerogels. However, it has been proven that the photocatalytic properties of TiO₂ aerogels containing an appropriate ratio of anatase TiO2 and rutile TiO₂ are stronger than that of TiO₂ aerogels containing only anatase TiO₂ (Figure 5(c)), which is mainly related to the mixed crystal effect achieved by these two crystalline phases [51]. Different crystal types of TiO₂ have more defects during the connection of structural elements, and more traps to capture photogenerated electrons and holes, thereby increasing the photocatalytic efficiency. Also, due to the difference in the energy levels of the conduction band and valence band of anatase TiO₂ and rutile TiO₂, photogenerated electrons formed by light excitation tend to diffuse from rutile TiO₂ to anatase TiO₂, while photogenerated holes are just the opposite, thereby reducing the recombination probability of electron-hole pairs, and realizing the effective separation of photogenerated carriers, which macroscopically shows that the photocatalytic properties of TiO2 aerogels are improved, as displayed in Figure 5(d).

In addition, the other factor that determines the photocatalytic properties of TiO_2 aerogels is the particle size of anatase TiO_2 nanoparticles and rutile TiO_2 nanoparticles as basic building blocks or secondary particles. As a typical N-type semiconductor, the particle size of

TiO₂ nanoparticles is generally smaller than the thickness of the space charge layer, so all the effects of the space charge layer can be ignored [52,53]. For instance, the diffusion rate of electrons from within the particle to the surface in 10 nm TiO₂ nanoparticles is four orders of magnitude higher than that of the same type of 1 µm TiO₂ nanoparticles. Therefore, the smaller the particle size, the shorter the time for photogenerated electrons to diffuse from within the particle to the surface, and the smaller the recombination probability of electrons and holes, which is helpful to improve the photocatalytic efficiency. Also, when the particle size of TiO₂ nanoparticles is smaller than a certain value, they can produce size quantum effects that have different properties from crystalline TiO₂ macroscopic materials [54]. As a result, electrons and holes are respectively confined in small-sized potential wells, so that the energy levels of the conduction band and the valence band are changed from continuous to separated, resulting in a wider bandgap between the two. In this case, the potential of the conduction band becomes more negative, and the potential of the valence band becomes more positive, which increases the energy of photogenerated electrons and holes. Thus, the redox capacity of TiO2 aerogels is enhanced, and their photocatalytic properties are significantly improved.

8 — Xin Long et al. DE GRUYTER

In addition, the smaller the particle size of anatase TiO₂ nanoparticles and rutile TiO₂ nanoparticles in TiO₂ aerogels, the larger the specific surface area of TiO2 aerogels [55,56]. On the one hand, the increase in the specific surface area can rapidly increase the number of surface atoms in TiO₂ aerogels, thereby improving the light absorption efficiency, increasing the concentration of surface photogenerated electron-hole pairs, and also accelerating the progress of the photocatalytic reaction. On the other hand, the increase in the specific surface area causes the surface bond state and electronic state to be different from the inside, and the uneven coordination of surface atoms increases the number of surface active sites, which enhance the adsorption capacity of TiO2 aerogels for reactants, and also increase the probability of the photocatalytic reaction.

4 TiO₂ aerogel composite photocatalysts for environmental treatment

4.1 Mechanism of photocatalysis

Photocatalytic reaction refers to the photochemical redox process that occurs between photocatalysts and their surface adsorbents, such as H₂O, organic matters, high-valent metal salts, etc., with the participation of light, which is essentially a free radical reaction [27,57]. As a typical N-type semiconductor, TiO₂ contains a full valence band, an empty conduction band, and a bandgap between the two in its electronic structure [29]. When the photon energy absorbed by the TiO2 reaches or exceeds the bandgap energy, the electrons in the valence band are excited to the conduction band, and holes are formed in the original position, that is, electron-hole pairs are formed. Generally, the holes in the valence band and the electrons in the conduction band are very easy to recombine and lose energy in the form of light energy or heat – equations (1) and (2) [58]. When trapping agents or surface states exist, the effective separation of electron-hole pairs can be achieved. Thereinto, holes are excellent oxidants with extremely high reactivity and are the main part of light quantum energy. They generally react with H₂O and OH⁻ on the surface of the TiO₂ to form active hydroxyl group (OH) with strong oxidizing properties - equations (3) and (4) [59]. As a free radical containing unpaired electrons, the 'OH has a reaction

energy of 402,800 kJ/mol, which is much higher than the bond energy of chemical bonds in various substances, such as 607.0 kJ/mol of the C−C bond, 338.32 kJ/mol of the C−H bond, 347.1 J/mol of the H−S bond, 1071.1 kJ/mol of the C≡O bond, and 339.0 kJ/mol of the N−H bond, *etc.*, so it can react with almost all organic pollutants and most inorganic pollutants (Figure 6(a)) [37].

The reaction speed of the 'OH is very high, only depends on its diffusion speed in the reaction system, and the reaction mechanism involved is mainly the addition reaction on the unsaturated double bonds and triple bonds, the substitution of H atoms, the transfer of electrons, *etc.* Studies have shown that the 'OH plays a leading role in the photocatalytic degradation [60,61].

Generally, the electrons first react with the O_2 adsorbed on the surface of the TiO_2 photocatalysts to generate superoxide radical $(\cdot O_2^-)$ – equation (5). Subsequently, the $\cdot O_2^-$ participates in a series of redox reactions and finally generates hydrogen peroxide (H_2O_2) (equations (6)-(8)) [52,62]. Although the oxidation potential of the H_2O_2 is lower than that of the TicologianOH, it can still play a role in the photocatalytic reaction. Also, the TicologianOH another source of the TicologianOH, as shown in equation (9) [63]. Therefore, through the above reaction steps, the TicologianOH and TicologianOH and TicologianOH and TicologianOH and TicologianOH are the photocatalytic reaction can react with various pollutants to finally produce TicologianOH, TicologianOH, TicologianOH, and TicologianOH, as a shown in equation (9) [63]. Therefore, through the above reaction steps, the TicologianOH and TicologianOH and TicologianOH, as a shown in equation (9) [63]. Therefore, through the above reaction steps, the TicologianOH and TicologianOH and TicologianOH are the photocatalytic reaction can react with various pollutants to finally produce TicologianOH, as a shown in equation (9) [63].

$$TiO_2 + h\nu \rightarrow e^- + h^+, \tag{1}$$

$$e^- + h^+ \rightarrow N + Energy (hv' < hv \text{ or heat}),$$
 (2)

$$h^+ + OH^- \rightarrow \cdot OH$$
, (3)

$$H_2 O+ h^+ \rightarrow \cdot OH + H^+,$$
 (4)

$$O_2 + e^- \rightarrow \cdot O_2^-,$$
 (5)

$$^{\circ}O_{2}^{-} + H_{2}O \rightarrow ^{\circ}OOH + OH^{-},$$
 (6)

$$2 \cdot 00H \rightarrow H_2O_2 + O_2,$$
 (7)

$$OOH + H_2O + e^- \rightarrow H_2O_2 + OH^-,$$
 (8)

$$H_2O_2 + e^- \rightarrow \cdot OH + OH^-.$$
 (9)

4.2 Kinetic principles of photocatalysis

The study of the photocatalytic reaction kinetics of ${\rm TiO_2}$ aerogels is not only a basic requirement for rational design of material components and structures, but also a way to better understand the abovementioned reaction mechanism. Based on the same basis of the photocatalytic reaction of

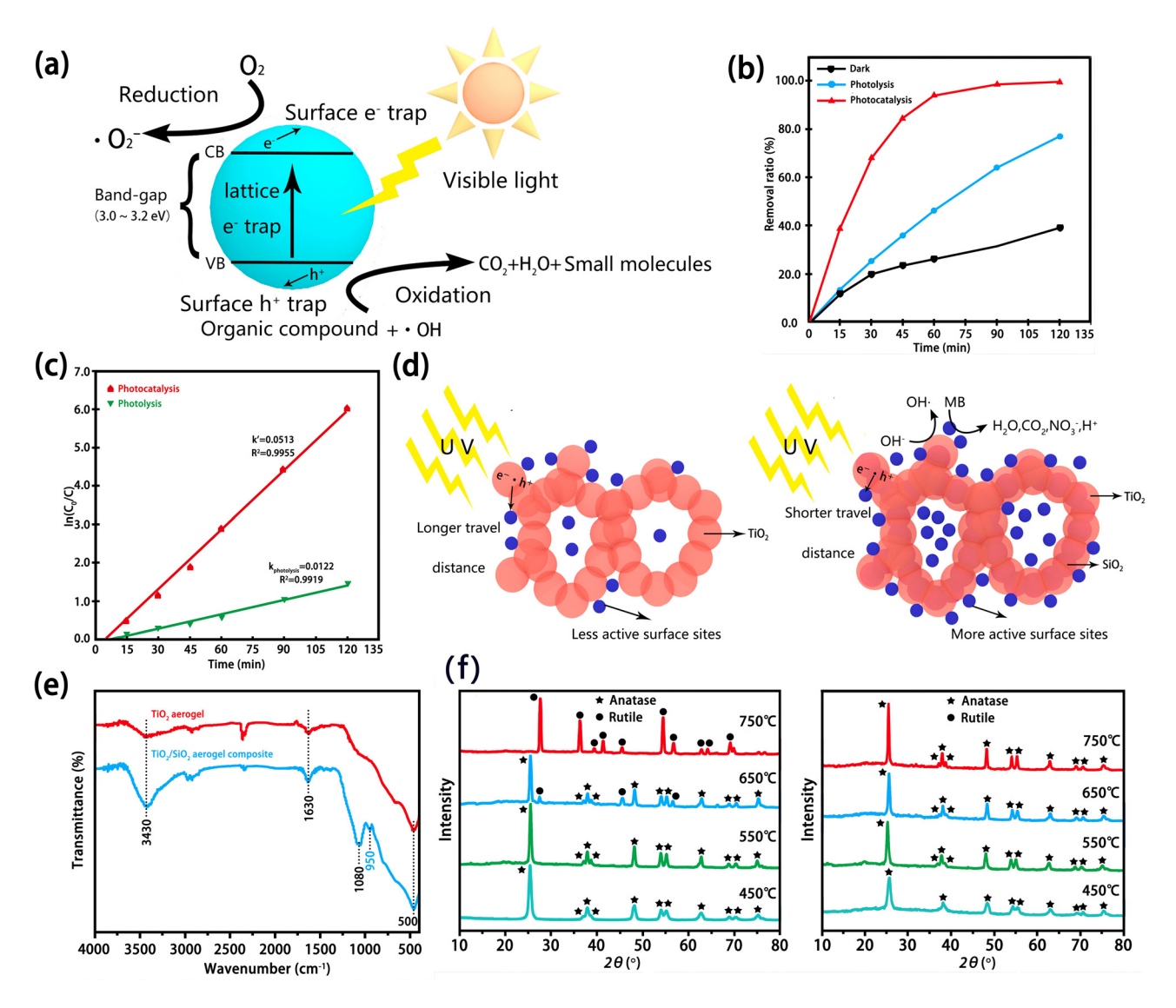


Figure 6: (a) Schematic diagram of the photocatalytic reaction process of nano-TiO₂; (b) photocatalytic degradation, photolysis, and adsorption curves of methylene blue by the TiO_2-SiO_2 aerogel; (c) linear relationship between CO/C and time for photocatalysis and photolysis of the TiO_2-SiO_2 aerogel; (d) schematic representation of the photocatalytic decomposition mechanism of methylene blue by the pure TiO_2 aerogel and the TiO_2-SiO_2 composite aerogel; (e) FTIR spectra of the pure TiO_2 aerogel and the TiO_2/SiO_2 aerogel composite calcined at 500°C; and (f) XRD patterns of pure TiO_2 aerogels and TiO_2/SiO_2 aerogel composites calcined at different temperatures. (b) and (c) Modified with permission from ref. [64]. Copyright 2009, Elsevier. (e) and (f) Modified with permission from ref. [74]. Copyright 2011, Elsevier.

 ${
m TiO_2}$ aerogels and their composites, Luo *et al.* [64], Sadrieyeh and Malekfar [23], and Shi *et al.* [65] have conducted indepth studies on the photocatalytic kinetics of the ${
m TiO_2}/{
m SiO_2}$ composite aerogel, the Au/Ag nanoparticles doped ${
m TiO_2}/{
m carbonaceous}$ aerogel, and the biomass-derived ${
m TiO_2}/{
m carbonaceous}$ aerogel composite, respectively, and reached a consistent conclusion: the photocatalytic reaction of ${
m TiO_2}$ aerogels follows the Langmuir–Hinshelwood (L–H) kinetic model. Take the study of Luo *et al.* as an example. Under the condition of homogeneous mixed transportation, they made the following assumptions in consideration of the possible mass

transmission effects involved: (1) the O_2 in the solution is always saturated and (2) the concentration of the reactant at the interface is no different from that in the solution. Based on this, the reaction rate formula shown in equation (10) can be obtained.

$$r = \frac{kKC}{1 + KC},\tag{10}$$

where C is the concentration of the reactant, k is the apparent reaction rate constant, and K is the equilibrium adsorption constant of the reactant. By taking the

reciprocal of both sides of equation (10), the kinetic constants *k* and *K* can be calculated to form linear equation (11).

$$\frac{1}{r} = \frac{1}{kK} \cdot \frac{1}{C} + \frac{1}{k}.$$
 (11)

When the reactant is at a low concentration, the final quasi-first-order kinetic equation (12) is obtained by integrating equation (11).

$$\ln\left(\frac{C_0}{C}\right) = kKt = k't,$$
(12)

where k' is the apparent quasi-first-order reaction rate constant.

In the research of Luo et al. [64], the pseudo-firstorder L-H kinetic model is assumed to be consistent with the kinetic model of the photocatalytic degradation of methylene blue by the TiO₂/SiO₂ composite aerogel. If this assumption is true, $In\left(\frac{C_0}{C}\right)$ and t form a linear relationship with a slope equal to k'. According to the characterization results of the removal of methylene blue by the TiO₂/SiO₂ composite aerogel under the conditions of darkness, photolysis, and photocatalysis, a fitting result showing a good linear relationship between $In(\frac{c_0}{c})$ and t is obtained (Figure 6(b)), which is consistent with the assumption that the degradation of methylene blue by the TiO₂/SiO₂ composite aerogel follows the quasi-firstorder reaction kinetics, and can be represented by a simplified L-H model. Meanwhile, the photolysis linearization curve ($R^2 = 0.9919$) shows that the photolysis of methylene blue is a simple first-order reaction, and the comparison of the reaction rate constants of photocatalysis (k = 0.0513) and photolysis ($k_{\text{photolysis}} = 0.0122$) also confirms that the photocatalysis plays a leading role in the degradation of methylene blue (Figure 6(c)).

4.3 TiO₂/SiO₂ composite aerogels

Since Kistler [66] used the supercritical drying process to prepare SiO_2 aerogels for the first time in 1931 and opened up a new field of aerogels, SiO_2 aerogels have experienced a total of more than 80 years of development from the vigorous development period of the last century to the stable development period of this century [67,68]. There is no doubt that the advanced technology formed during the development of SiO_2 aerogels has driven the development of TiO_2 aerogels in this century. Especially in recent years, the design and preparation of TiO_2/SiO_2 composite aerogels has become one of the main research directions to overcome the limitations of TiO_2 aerogels.

Compared with TiO2 aerogels, SiO2 aerogels have more significant structural characteristics of aerogels, such as larger specific surface area, higher porosity, finer nanoparticles, higher light transmittance, etc. [40,69,70]. As mentioned earlier, the larger specific surface area can increase the light absorption efficiency of TiO2 aerogels and the number of active sites formed due to the uneven coordination of surface atoms. The higher porosity means that TiO₂ aerogels have stronger adsorption and holding capacity for reactants, which is conducive to increasing the concentration of reactants in the active centers and improving the probability of reactions. The finer nanoparticles can effectively increase the specific surface area and form quantum size effects required for photocatalysis, etc. The higher light transmittance represents a wider light excitation space, so the total area of TiO₂ aerogels excited by light increases and the number of active centers formed increases (Figure 6(d)).

It is for the above reasons that SiO₂ aerogels have great potential to be applied as a kind of nano-catalyst carrier with superior performance, and TiO2 nanomaterials including TiO2 aerogels can rely on the structural characteristics to maximize the photocatalytic properties, which is the first design form of TiO₂/SiO₂ aerogel composites with SiO₂ aerogels as the main body and TiO₂ nanomaterials as the guest. Generally, there are two ways to realize this type of TiO_2/SiO_2 composite aerogels. One is to introduce crystallized TiO2 nanoparticles into the SiO₂ aerogels at the formation stage [71], and the other is to immerse the selected Ti-containing precursors into the already formed SiO2 aerogels' framework network to combine the two to form composite aerogels [72]. Although the content of TiO₂ crystalline phases in this type of TiO₂/SiO₂ composite aerogels is lower than that of pure TiO₂ aerogels, their photocatalytic properties are more excellent. As the content of TiO₂ crystalline phases increases within a certain range, their photocatalytic properties can be continuously strengthened [72].

For instance, under the irradiation of 250 W UV light source, the TiO_2/SiO_2 composite aerogels (10 mg) prepared by immersing the formed SiO_2 wet gel in the partially hydrolyzed titanium n-butoxide precursor for 5, 10, and 15 times, respectively, achieved 55, 78, and 92% degradation rates (100 min) for methylene blue solution (20 mg/L, 40 mL) [73]. Under the irradiation of UV light source (254 nm), the TiO_2/SiO_2 composite aerogels (0.277 g) prepared by adding SiO_2 aerogels into the TiO_2 sol with concentrations of 0.43, 0.75, and 1.20 mol/L by ultrasonic vibration produced about 53, 80, and 54% degradation rates (200 min) for rhodamine B solution (1.0 \times 10⁻⁴ mol/L, 30 mL), respectively. In the research, the photocatalytic

properties of the composite aerogel with the highest TiO₂ content decreased, which was mainly related to the weakening of the structural characteristics of the SiO2 aerogel caused by the excessive loading of TiO₂ aerogels [72]. Wang et al. [74] prepared a TiO₂/SiO₂ composite aerogel by adding the SiO₂ aerogel to the hydrolysate of Ti-containing precursor, and systematically studied the effect of experimental conditions on the photocatalytic properties. The results showed that the photocatalytic properties of the composite aerogel were the best when the pH value was 4.82, the dosage was 8.0 g/L and the temperature was 20°C, and the degradation rate of 2-sec-butyl-4.6-dinitrophenol (DNBP) (41.90 mg/L, 75 mL) reached 95% (240 min) under sunlight irradiation (0.562 kW/m²). Under the irradiation of a sunlight simulator (132.7 mW/cm²) with a height of 10.16 cm, an inner diameter of 7.62 cm, and an outer diameter of 5.08 cm, the TiO₂/SiO₂ composite aerogel obtained by immersing the anatase TiO₂ aerogel (10 mg/cm²) into the about-to-gel SiO2 sol on a 1 cm × 1 cm glass substrate for nano-gluing reaction achieved the highest degradation rate of 94.3% (60 min) for methylene blue solution (4 mg/L) [64].

In addition, in order to adjust the content and ratio of TiO₂ and SiO₂ in TiO₂/SiO₂ composite aerogels more conveniently and flexibly, and try to make the two composites in the form of chemical bonding, researchers are inclined to use co-sol-gel to make Ti-containing precursors and Si-containing precursors react synchronously to construct the structural framework of TiO₂/SiO₂ composite aerogels, so as to achieve the structural uniformity of the two on the atomic scale, which is another type of TiO₂/SiO₂ composite aerogels [75,76]. Thereinto, in addition to the advantages of structural characteristics, SiO₂ aerogels can also affect the photocatalytic process and structural stability of TiO2 aerogels to a certain extent. SiO₂, as a charge transfer catalyst, can affect the transfer process of photogenerated electrons and holes to the surface, thereby inhibiting their recombination. Because anatase TiO₂ has an octahedral coordination structure, the existence of SiO2 can lead to the unbalanced distribution of charge, resulting in the formation of Brønsted acid sites. As a result, more OH⁻s are adsorbed on the surface to achieve charge balance, which not only can further capture holes and improve the separation efficiency of electron-hole pairs, but also promote the generation of OHs, thereby enhancing the photocatalytic properties of TiO₂ aerogels [64]. Also, the composite of SiO₂ aerogels can effectively inhibit the transformation of anatase TiO₂ to rutile TiO₂, which is mainly due to the formation of Ti-O-Si bonds which stabilize nearby anatase TiO2 (Figure 6(e) and (f)) [74]. The SiO₂ crystal lattice locks the Ti-O species on the interface of the TiO₂ region,

preventing the nucleation process necessary for the transformation of anatase TiO₂ to rutile TiO₂, which not only ensures the composition of a high proportion of anatase TiO₂, but also ensures the realization of the mixed crystal effect. However, in the former type of TiO₂/SiO₂ composite aerogels, SiO₂ aerogels and TiO₂ nanomaterials including TiO₂ aerogels are mostly combined by physical means such as impregnation, coating, embedding, *etc.*, thereinto the influence of SiO₂ aerogels on the photocatalytic process and the structural stability of TiO₂ crystalline phases is very weak. Comparing the research history of the two types of TiO₂/SiO₂ composite aerogels, it can be found that the design of the second type of composite form is more concerned.

For instance, under the irradiation of 3 W \times 10 W OVA lamp sources, the degradation rate of the TiO₂/SiO₂ composite aerogel (0.5 g, mass ratio of TiO₂/SiO₂ is 1.8) to gas phase acetaldehyde (2,000 ppmv) in a cuboid reactor $(220 \text{ mm} \times 125 \text{ mm} \times 80 \text{ mm})$ reached 82% (20 min), while the Degussa-P25 used in the control group produced only 52% degradation rate under the same conditions [77]. Under the irradiation of a high-pressure mercury lamp (350-450 nm), the adsorption rate of the TiO₂/SiO₂ composite aerogel (0.1 g, molar ratio of Ti/Si is 4) prepared by sol pre-modification to rhodamine B solution $(9.8 \times 10^{-6} \text{ mol/L})$ 20 mL) reached 89.4% within 1 h, and the total photocatalytic/adsorption removal rate reached 96.5% within 10 h [41]. The superhydrophobic TiO₂/SiO₂ composite aerogel (0.1 g, hydrophobic angle is 165°, and molar ratio of Ti/Si is 1:1) produced a 35% removal rate for rhodamine B solution (10 mg/L, 100 mL) when it was not exposed to light, and a 74.5% (100 min) removal rate was obtained when it was irradiated by an iodine tungsten lamp (125 W) through the synergistic effect of photocatalysis and adsorption, while the Degussa-25 selected in the control group only produced a removal rate of 22% under the same conditions with light irradiation [43]. Under the irradiation of 8 W ultraviolet light source, the mineralization rates of TiO₂/SiO₂ nanocomposite aerogel catalysts (0.2 g, molar ratio of Ti/Si is 1:1 and 1:4, respectively) for trinitrotoluene reached 99 and 93% (3.5 h), respectively [78]. In addition, the photocatalytic application effects of TiO₂/SiO₂ composite aerogels used in environmental treatment are shown in Table 1.

4.4 Metal dopants modified TiO₂ aerogels

Metal dopants are commonly used means to improve the photocatalytic properties of TiO₂ aerogels. According to the differences in process methods and modification effects,

Table 1: Summary of degradation effects of TiO₂-SiO₂ aerogel composites on various environmental pollutants

Catalysts	Usage amount	Condition	Target	Time	Removal efficiency (%)	Ref.
TiSi-1	10 mg	250 W UV light	Methylene blue (40 mL, 20 mg/L)	100 min	92	[73]
TiSi-1	0.277 g	254 nm UV light	Rhodamine B (30 mL, 1.0 \times 10 ⁻⁴ mol/L)	200 min	80	[72]
TiSi-1	0.6 g	0.562 kW/m² sunlight	DNBP (75 mL, 41.90 mg/L)	240 min	95	[74]
TiSi-1	10 mg	132.7 mW/cm ² sunlight simulator	Methylene blue (4 mg/L)	60 min	94.3	[64]
TiSi-2	/	16 W UV light	Glyphosate (500 mL, 20 mg/L)	180 min	100	[28]
TiSi-2	10 mg	765 W/m² visible light	Methylene blue (10 mL, 10 μM)	12 h	>95	[71]
TiSi-2	0.142 g	$5 \text{ nm} \times 365 \text{ nm fluorescent black}$ lamps	Gas trichloroethylene (113 ppm)	/	19.3	[76]
TiSi-2	0.2 g	8 W UV light	TNT (700 mL, 100 ppm)	3.5 h	99	[78]
TiSi-2	125 μg/mL	150 W mercury vapor lamp	Methylene blue (50 μM)	3 h	82	[79]
TiSi-2	125 μg/mL	150 W mercury vapor lamp	Salicylic acid (500 μM)	3 h	30	[79]
TiSi-2	0.12 g	100 W mercury lamp	Methylene blue (200 mL, 48 mg/L)	70 min	96	[75]
TiSi-2	0.5 g	$3 \times 10 W$ UVA lamps	Acetaldehyde (2.2 L, 2,000 ppmv)	120 min	100	[77]
TiSi-2	5 g	$2 \times 10 W$ UVA lamps	NO _x (0.075 L, 1 ppmv)	180 min	91	[77]
TiSi-2	0.1 g	125 W iodine tungsten lamp	Rhodamine B (100 mL, 10 mg/L)	100 min	74.5	[43]
TiSi-2	0.1 g	350-450 nm mercury lamp	Rhodamine B (20 mL, 9.8 \times 10 ⁻⁶ mol/L)	10 h	96.5	[41]
TiSi-2	1 mg/mL	40 W UV lamp	Methylene blue (5 mg/L)	120 min	89	[80]

Note: TiSi-1 represents the first type of TiO_2/SiO_2 composite aerogels, TiSi-2 represents the second type of TiO_2/SiO_2 composite aerogels, and DNBP is 2-sec-butyl-4,6-dinitrophenol.

they can be divided into doping modification of metal ions and local surface plasmon resonance modification of metal nanoparticles [25,56]. Generally, the modification effects of metal ions on TiO2 aerogels are mainly reflected in the following three aspects: (1) inhibit the recombination of photogenerated electron-hole pairs [81], (2) appropriately reduce the bandgap and broaden the response range to visible light [82], and (3) promote the formation of crystalline TiO₂ and inhibit the transformation of anatase TiO₂ [83]. Up to now, representative transition metal ions such as Zn²⁺, Fe³⁺, etc., and rare earth metal ions such as La³⁺, Nd³⁺, Eu³⁺, etc., have been widely used in the modification of TiO₂ aerogels. For instance, the doping of Zn²⁺ effectively promotes the formation of crystalline TiO₂ in TiO₂ aerogels, and as the Zn/Ti molar ratio increases in the range of 0-7%, the promotion effect is more obvious (Figure 7(a)) [82]. The doping of Fe $^{3+}$ can reduce the lattice constant c of anatase TiO_2 in the TiO_2 aerogel while maintaining a unchanged, which inhibits the growth process of crystalline phases when external conditions change, such as temperature rise (Figure 7(b)) [83].

Based on the theory established by Rodriguez *et al.* [84], when the radius of doped metal ions is different from that of Ti⁴⁺ (0.068 nm), lattice distortion will be caused, and the resulting stress field will definitely inhibit

the movement of grain boundaries, thereby preventing the occurrence of phase transition. Zn2+ has a large ionic radius (0.088 nm) and is difficult to enter the lattice of TiO₂. Therefore, low-concentration Zn²⁺ doping is easy to precipitate ZnO clusters on the surface of TiO2 aerogels and become the nucleation center of rutile TiO2, thereby reducing the temperature of crystalline phase transition. The ionic radius of Fe3+ (0.069 nm) is relatively close to that of Ti⁴⁺, which can easily replace Ti⁴⁺ in the TiO₂ lattice or enter the lattice gap to form a uniform distribution in TiO₂ aerogels, and thus become the center of preferential nucleation of rutile TiO₂, which also helps to reduce the temperature of crystalline phase transition. Meanwhile, Guidi et al. [85] found that there are fractures of Ti-O bonds in the transformation from anatase TiO2 to rutile TiO₂, which causes the increase in mobility and promotes the growth of crystalline grains, and the doping of metal ions can just affect the formation mechanism of rutile TiO₂, which makes the nucleation site of rutile TiO₂ in TiO₂ aerogels transfer from the junction of anatase TiO2 to the surface, resulting in excessive accumulation of rutile TiO2 nucleation centers on the surface, which reduces the growth rate and delays the formation process. As a result, the particle size of TiO₂ is reduced, which in turn maintains the stability of anatase TiO₂. Also, the growth of a small

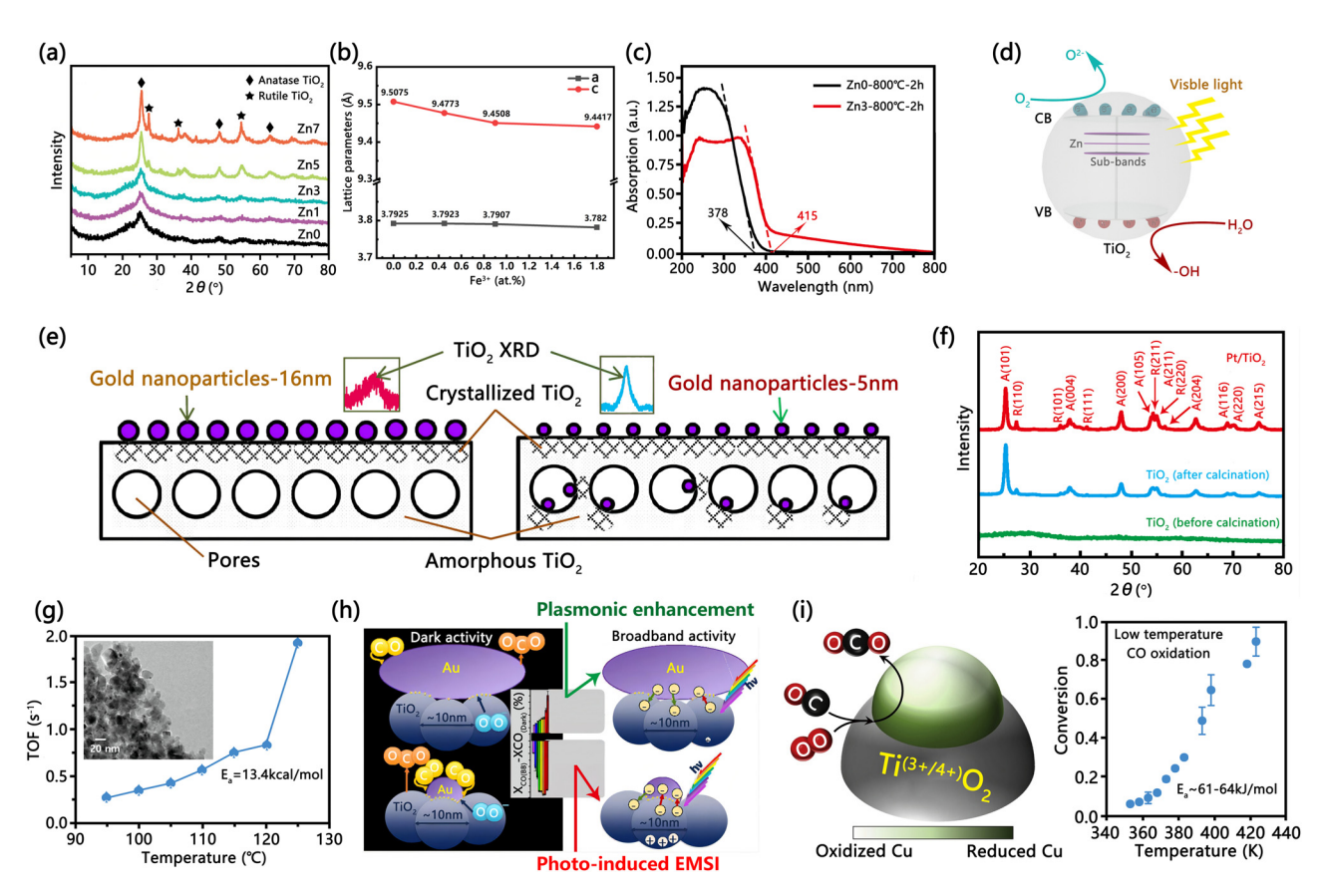


Figure 7: (a) XRD patterns of heat-treated Zn²⁺ doped TiO₂ aerogels at 800°C for 2h with different mole fractions of Zn; (b) effects of the Fe³⁺ doping with different molar fractions on lattice parameters *a* and *c* of anatase TiO₂ in TiO₂ aerogels; (c) diffuse reflectance spectra of the ZnO-800°C-2h and the Zn3-800°C-2h; (d) the schematic diagram of synergistic effect between TiO₂ and Zn photocatalytic system in the Zn doped TiO₂ aerogels under visible light irradiation; (e) graphical illustration of the difference in modification of TiO₂ aerogels by Au nanoparticles with different particle sizes; (f) XRD patterns of TiO₂ aerogels before and after calcination and the Pt/TiO₂ aerogel after calcination; (g) variation curve of turnover frequency with temperature of the catalytic activity for CO oxidation of the Pt nanoparticles surface-modified TiO₂ aerogel; (h) competitive effect of the favorable plasma enhancement of Au nanoparticles and the unfavorable photo-induced EMSI on the catalytic activity of TiO₂ aerogels for CO in dark and broadband environments; and (i) schematic diagram of the effect of TiO₂ aerogels on Cu nanoparticles and changing relationship of temperature on the conversion rate of CO by the Cu nanoparticles surface-modified TiO₂ aerogel. (a) and (c) Modified with permission from ref. [82]. Copyright 2018, IOP. (b) Modified with permission from ref. [83]. Copyright 2009, Springer. (e) Reproduced with permission from ref. [57]. Copyright 2013, Elsevier. (f) and (g) Modified with permission from ref. [56]. Copyright 2018, Springer. (h) Reproduced with permission from ref. [96]. Copyright 2020, American Chemical Society. (i) Reproduced with permission from ref. [98]. Copyright 2019, Elsevier.

amount of rutile TiO_2 on the surface of anatase TiO_2 is also conducive to the realization of the mixed crystal effect.

Furthermore, transition metal ions replace Ti^{4+} in the TiO_2 lattice, enter the lattice gap, precipitate with metal oxides, *etc.*, which can lead to the generation of point defects, and the resulting Coulomb effect increases their separation efficiency by trapping electrons or holes. Meanwhile, the charged metal ions themselves can become trapping potential wells for electrons or holes. Taking Fe^{3+} doping as an example [86], although its energy level is above the conduction band energy level of rutile TiO_2 , it is closer to the conduction band of TiO_2 . Therefore, a deep potential capture well for trapping holes can be formed to reduce the

recombination probability of electron—hole pairs. Under the irradiation of 8 W/cm² UV light, the Fe³+ (3% mole fraction) doped TiO₂ aerogel (16.6 g/L) achieved a 85.1% degradation efficiency (120 min) for salicylic acid (5 × 10 $^{-4}$ mol/L), and the photocatalytic effect produced was 1.2 times that of the pure TiO₂ aerogel and 6 times that of the Degussa-P25 under the same conditions [83]. Under the sunlight, the Fe³+ (3% mole fraction) doped TiO₂ aerogel (0.25 g/L) synthesized with ionic liquid as a template achieved about 95% degradation rate (120 min) for reactive blue dye (40 mg/L, 200 mL), which was higher than 88% of the pure TiO₂ aerogel and 35% of the Degussa-P25 under the same conditions [87].

Regarding the regulation of energy band structure, the doping of metal ions can introduce impurity state energy levels in the bandgap of TiO2 to narrow the bandgap, which causes the red shift of the light absorption sideband caused by electrons from the valence band to the conduction band, and broadens the light absorption range of TiO2 aerogels. Take Zn2+ doping as an example [82], the adsorption edge wavenumber of the pure TiO₂ aerogel treated at 800°C for 2 h (Zn-0-800°C) was 378 nm. After doping with 3% mole fraction of Zn²⁺ (Zn-3-800°C), its adsorption edge wavenumber was increased to 415 nm, indicating that the doping of Zn²⁺ lead to the occurrence of red shift (Figure 7(c)). This is mainly due to the substitution of Zn²⁺ for Ti⁴⁺ which introduces impurities and defect levels into the bandgap of TiO2, and the resulting sub-forbidden band reduces the bandgap energy and improves the photocatalytic efficiency (Figure 7(d)). In the 2h non-light adsorption reaction, the adsorption efficiency of the Zn-3-800°C (0.1 g) on rhodamine B solution (10 mg/L, 50 mL) was 84.28%, and the adsorption efficiency of the Zn-0-800°C and Degussa-P25 were 83.98 and 2.66% under the same conditions, respectively, which was mainly due to the specific surface area of Degussa-P25 (about 50 m²/g) was much lower than that of the Zn- $3-800^{\circ}$ C (614.7 m²/g) and the Zn-0-800°C (522.0 m²/g). Subsequently, under the irradiation of 300 W tritium lamp, the photocatalytic efficiency of the Zn-3-800°C reached 98.77% (2h), which was higher than 95.41% of the Zn-0-800°C and 91.87% of the Degussa-P25.

In addition to the above modification mechanism, rare earth metal elements have unique incompletely filled 4f orbitals and empty 5d orbitals, and the 4f electrons of their ions can undergo energy level transitions between the f-f configuration or between the f-d configuration, causing the distortion of the TiO₂ lattice, thereby making the lattice O atoms easy to fall off to form O vacancies, which improves the adsorption capacity of TiO₂ aerogels to the reactants and increases the number of OH-s on the surface to form more 'OHs [88]. Therefore, the photocatalytic properties of TiO₂ aerogels are also improved. For instance, in the 6 h adsorption study, the adsorption capacities of salicylic acid $(2 \times 10^{-4} \text{ M}, 3 \text{ mL})$ on the 0, 0.72, 14.8, 2.71, and 5.30 wt% Eu₂O₃ doped TiO₂ aerogels $(7 \pm 0.5 \,\mathrm{mg})$ were <1, 33.5, 35.3, 33.2, and 31.8 μ mol/L, respectively. After 60 min irradiation of 1,000 W Xe-Hg lamp, their photocatalytic degradation efficiency for the salicylic acid reached 4.4 ± 2 , 84.8 ± 4 , 78.1 ± 4 , 79.6 ± 4 , and 100%, respectively. In the research, the strong adsorption effect of Eu₂O₃ doping on TiO₂ aerogels has become a key factor in determining the photocatalytic properties [89].

The rapid development of the localized surface plasmon resonance (LSPR) provides a new and effective method for improving the catalytic properties of photocatalysts [90-92]. Generally speaking, there are two mechanisms for the influence of plasma metals on the photocatalytic properties of TiO₂ aerogels: (1) hot electron transfer mechanism and (2) near-field electromagnetic mechanism. In the mechanism (1), plasma-induced electrons in metal nanoparticles are transferred to the conduction band of TiO2. Thus, reduction and oxidation reactions occur on the surface of TiO2 and plasma metal nanoparticles, respectively [93]. In the mechanism (2), plasma metal nanoparticles act as a light concentrator to amplify the intensity of light irradiation, and ultimately promote the generation of electron-hole pairs near the metal nanoparticles, which usually requires an overlap between the light radiation source, the LSPR of metal nanoparticles and the absorption spectrum of TiO2 [94]. In addition, metal nanoparticles can also have a certain effect on the crystalline structure of TiO2, which is similar to the doping effect of metal ions.

The modification effect of metal nanoparticles largely depends on their type, size, concentration, and doping methods (surface modification or uniform doping) [57]. Meanwhile, the structural characteristics of ${\rm TiO_2}$ aerogels, such as large specific surface area, high porosity, the 3-dimensional connected nanoporous structure, etc., also provide the structural basis for the loading of metal nanoparticles, which can prevent the aggregation of entrained metal nanoparticles and make them more stable in different environments.

Under the irradiation of 6×6 W radiation sources, 5 nm (0.12, 0.19, and 0.22 wt%) and 16 nm (0.14, 0.24, and 0.34 wt.%) Au nanoparticles surface-modified TiO₂ aerogels produced reaction rates (7,000 s) of 9.1, 12.6, $46.4 \,\mu\text{mol/(L s)}$ and $6.5, 6.5, 23.2 \,\mu\text{mol/(L s)}$ for salicylic acid (0.5 mmol/L), respectively, indicating that Au nanoparticles with smaller particle size and higher concentration produced stronger LSPR. Thus, the bandgap of TiO₂ was reduced, and the contact area with TiO₂ aerogels was increased, resulting in the increase in crystalline region and the formation of more extensive crystallization, as shown in Figure 7(e) [57]. The doping of Ag nanoparticles can produce impurity levels less than 3.3 eV in TiO₂ aerogels to reduce their Fermi energy level. As the Ag/Ti molar ratio increased from 1:50 to 1:10, the bandgap energy of the resulting Ag uniformly doped TiO2 aerogel also decreased from 3.26 to 3.15 eV, their photocatalytic antibacterial rates against E. coli and S. aureus have also been improved, and even the TiO2 aerogel with the lowest concentration of Ag nanoparticles also produced more than 90% antibacterial rates against the two

bacteria [95]. When Au and Ag nanoparticles were used for the modification of ${\rm TiO_2}$ aerogels simultaneously, their photocatalytic effect on salicylic acid was stronger than that achieved when they were modified separately, which was mainly due to the combination of the different plasma characteristics of Au and Ag nanoparticles to further enhance the photocatalytic properties of ${\rm TiO_2}$ aerogels, as demonstrated by Sadrieyeh and Malekfar [23].

In addition to the research on water treatment, TiO₂ aerogels modified by metal nanoparticles have also been studied in the catalytic oxidation of industrial CO, which not only depends on the active photochemical properties of TiO₂ aerogels, but also on the high activation energy of precious metal nanoparticles. The conversion rate of the 2.95 ± 0.83 nm Pt nanoparticles (3.8% mole fraction) surface-modified TiO2 aerogel (0.1 g) to CO in the test gas (4% CO, 10% O2, and balanced with He) with an hourly space velocity of 6,000 h⁻¹ in a quartz reactor reached 100% (125°C), which was much higher than 30% of the untreated TiO2 aerogel [56]. Pt nanoparticles not only played an important role in promoting the formation of crystalline phases, and the miscible composition of 90.2% anatase TiO2 and 9.8% rutile TiO2 was formed by heat treatment of the TiO₂ aerogel only at 500°C, but also showed a high activation energy of 13.4 kcal/mol in the catalytic oxidation of CO (Figure 7(f) and (g)). Pennington et al. [96] systematically studied the effect of the particle size, loading capacity, and interface intimacy of Au nanoparticles with TiO₂ aerogels on the activity of CO catalytic oxidation under dark and broadband irradiations, and came to the following conclusions: (1) compared with the surface modification, TiO₂ aerogels uniformly doped by Au nanoparticles limited the dispersion and agglomeration of Au nanoparticles to form a more intimate interface contact; (2) the excessive amount of Au nanoparticles increased the average particle size due to the occurrence of agglomeration, and also weakened the Au||TiO₂ intimacy; (3) in a dark environment, the conversion rate of the TiO₂ aerogel uniformly doped by Au nanoparticles to CO was higher than that of the surface-modified TiO₂ aerogel, and the smaller Au nanoparticles produced higher Au||TiO₂ intimacy to form a higher CO conversion rate; (4) under broadband irradiation, the catalytic activity of Au-TiO2 aerogels with high Au||TiO₂ intimacy was weakened, which was mainly due to the harmful light-induced electronic metal-support interaction exceeding the beneficial LSPR effect (Figure 7(h)), and the increase in the size of Au nanoparticles and the weakening of the Au||TiO₂ intimacy could alleviate this harmful effect. In the dark, the TiO2 aerogel uniformly doped by Au nanoparticles (10 mg) produced the highest CO conversion rate for the test

gas (1% CO, 20% O_2 , and 79% He) with a flow rate of 80 mL/min in a glass tube (3/8" OD, 0.22" ID), which was 94.4 \pm 0.7% (150°C).

The doping modification of TiO2 aerogels by Cu nanoparticles is a relatively special study. The low-valent Cu^{0/1+} has an activation energy equivalent to the abovementioned noble metals such as Au, Pt, etc., and it also has the advantages of wide sources and low cost. However, nano-scale Cu is easily oxidized to Cu²⁺ and is difficult to stabilize at Cu^{0/1+}, and this problem can be solved by the structural characteristics and active photochemical properties of TiO2 aerogels. The transfer of electrons generated by TiO2 aerogels to CuO with high work function is energetically favorable, and the formation of defects such as oxygen vacancies can form Ti³⁺ in TiO₂, which also helps to provide electrons to the loaded Cu nanoparticles. This charge transfer is highly concentrated at Cu||TiO₂ interfaces, effectively suppressing the formation of CuO [97]. In addition, the $TiCuO_x$ mixed phases formed on the interface area between Cu₂O <111> film and TiO₂ can stabilize the highly reactive Cu¹⁺ sites and limit the oxidation of Cu₂O. Conversely, the presence of Cu nanoparticles can improve the photocatalytic properties of TiO₂ aerogels through the LSPR, and the coexistence of the two achieves a synergistic effect of complementary advantages. The Cu nanoparticles (10 wt%) surface-modified TiO₂ aerogel (12.5 mg) achieved above 95% CO conversion efficiency for the mixed gas (8 vol% CO) with a flow rate of 50 mL/min (150°C) in a glass tube $(3/8^{\circ}OD, 0.22^{\circ}ID)$, and also achieved a high ratio of $Cu^{0/1+}$ Cu^{2+} of 1.7 and a high activation energy of 63.7 \pm 3.2 kJ/mol (Figure 7(i)) [98]. In addition, the summary of the photocatalytic effects achieved by metal dopants modified TiO₂ aerogels is shown in Table 2.

4.5 Non-metallic substance doped/composite TiO₂ aerogels

The atomic radius of non-metallic elements used for the doping modification of TiO_2 aerogels usually needs to be close to that of O atoms [99]. Also, in order to produce a better modification effect, the doped non-metallic elements also need to meet the following conditions: (1) a new energy level that fully overlaps the energy level of TiO_2 is generated in the bandgap of TiO_2 [100], (2) generation of charged defects such as O vacancies for the efficient separation of electron–hole pairs [30], and (3) reduce the conduction band energy level to achieve the improvement of photocatalytic properties [101]. Nowadays, C and N

16 — Xin Long et al. DE GRUYTER

Table 2: Summary of degradation effects of metal dopants doped TiO2 aerogels on various environmental pollutants

Catalysts	Usage amount	Condition	Target	Time	Removal efficiency (%)	Ref.
Zn ²⁺ -TA	100 mg	300 W xenon lamp	Rhodamine B (50 mL, 10 mg/L)	4 h	98.77	[82]
Fe ³⁺ -TA	16.6 g/L	250 W Hg lamp	Salicylic acid (5 \times 10 ⁻⁴ M)	120 min	≈85.1	[83]
Fe ³⁺ -TA	0.25 g/L	Sunlight	Reactive blue (200 mL, 40 mg/L)	120 min	95	[87]
Eu ₂ O ₃ -TA	$7\pm0.5\text{mg}$	1,000 W Xe-Hg lamp	Salicylic acid (3 mL, 2×10^{-4} M)	60 min	100	[89]
AuNPs@TA	/	6 × 6 W lamps	Salicylic acid (0.5 mM)	7,000 s	30	[57]
AgNPs-TA	100 ppm	Sunlight	Diluted bacteria – E. coli (1 mL)	24 h	99.86	[95]
AgNPs-TA	100 ppm	Sunlight	Diluted bacteria – S. aureus (1 mL)	24 h	99.85	[95]
Au/AgNPs@TA	4 mg	300 W xenon lamp	Salicylic acid (3 mL, 0.5 mM)	120 min	≈65	[23]
Au/AgNPs-TA	4 mg	300 W xenon lamp	Salicylic acid (3 mL, 0.5 mM)	120 min	≈62	[23]
PtNPs@TA	100 mg	125° C	6,000 h ⁻¹ mixed gas (4 vol% CO)	_	100	[56]
AuNPs-TA	35 mg	300 W xenon lamp	Rhodamine B (100 mL, 2.32 $\times 10^{-5}$ M)	30 min	100	[14]
CuNPs@TA	12.5 mg	150° C	50 mL/min mixed gas (8 vol% CO)	_	>95	[98]
Pdi ₂ NPs-TA	10 mg	15 W Osram lamp	p-nitrophenol (40 mL, 0.088 mM)	200 min	98	[60]
Au-modified TA	10 mg	150 W white light, 150°C	0.8 mL/min CO	_	94.4 ± 0.7	[96]

Note: - represents the uniformly doped and @ represents the surface decorated.

atoms have attracted much attention due to their similar atomic size as O atoms, smaller ionization energy, and higher stability, so they can be easily incorporated into the TiO₂ crystal lattice. Under the irradiation of 500 W UV light, the TiO₂–C hybrid aerogel (50 mg) synthesized by sol–gel and high-temperature calcination achieved a 99.6% degradation efficiency (180 min) for methylene blue solution (20 ppm, 50 mL), and produced a rate constant of 0.06 min⁻¹ which was 4.23 times that of the Degussa-P25 in the control group. In addition to the modification effects mentioned above, the high reactivity is also related to the formation of oxygen vacancies in the TiO₂ aerogel doped by C atoms, resulting in macropore scattering and high light absorption [30].

The doping modification of N atoms mainly depends on the substitution ratios of internal O atoms and surface O atoms in the TiO_2 lattice. Under the irradiation of 250 W high pressure mercury lamp, the N atoms doped TiO_2 aerogels (1.66 g) synthesized with urea and ammonia as nitrogen sources produced photon efficiencies ξ of 1.26×10^{-4} and 1.32×10^{-4} for salicylic acid solutions (5 \times 10⁻⁴ mol/L, 100 mL), respectively – equation (13). Meanwhile, the modification of urea and ammonia produced 15.9 and 6.6% of internal O atom substitutions and 0 and 6.3% of surface O atom substitutions, respectively, which reduced the bandgap of the TiO_2 aerogels from 3.04 and 2.97 eV to 2.80 and 2.86 eV, respectively [101].

 ξ = Salicylic acid moles reacted per time unit/Einstein absorbed per time unit. (13)

In addition to the doping modification, the compounding of non-metallic substances is a more commonly used modification method, and the composite form adopted is similar to the first type of $\text{TiO}_2/\text{SiO}_2$ composite aerogels introduced earlier, which is achieved by immersing or depositing TiO_2 nanomaterials including TiO_2 aerogels in other non-metallic nanomaterials to take advantage of their structural properties and intrinsic properties to maximize the photocatalytic properties.

At present, a variety of C nanomaterials have been widely used in the preparation of TiO₂-C composite aerogels. Under simulated sunlight of 100 mW/m², the TiO₂ aerogel/C foam composite (1 g/L) prepared by vacuum infiltration produced a 100% degradation rate (40 min) for rhodamine B solution (1 \times 10⁻⁵ mol/L). The existence of C foam not only becomes the skeleton support to overcome the weak mechanical properties of TiO₂ aerogels and make them suitable for long-term application (Figure 8(a)) but also becomes the electron storage pool for the separation of electron-hole pairs, and also expands the light response range and improves the light utilization efficiency of TiO2 aerogels [102,103]. The active functional groups and defects on the surface of C aerogels synthesized from biomass raw material, wintermelon, are very beneficial to the fixation and growth of TiO2 nanoparticles (Figure 8(b)). Under the irradiation of 500 W tungsten lamp, the as-prepared biomass-derived multifunctional TiO₂/C aerogel composite (10 mg) achieved the highest degradation rate of 82% (210 min) for methylene blue solution (40 mg/L, 40 mL), which was higher than 40% of the

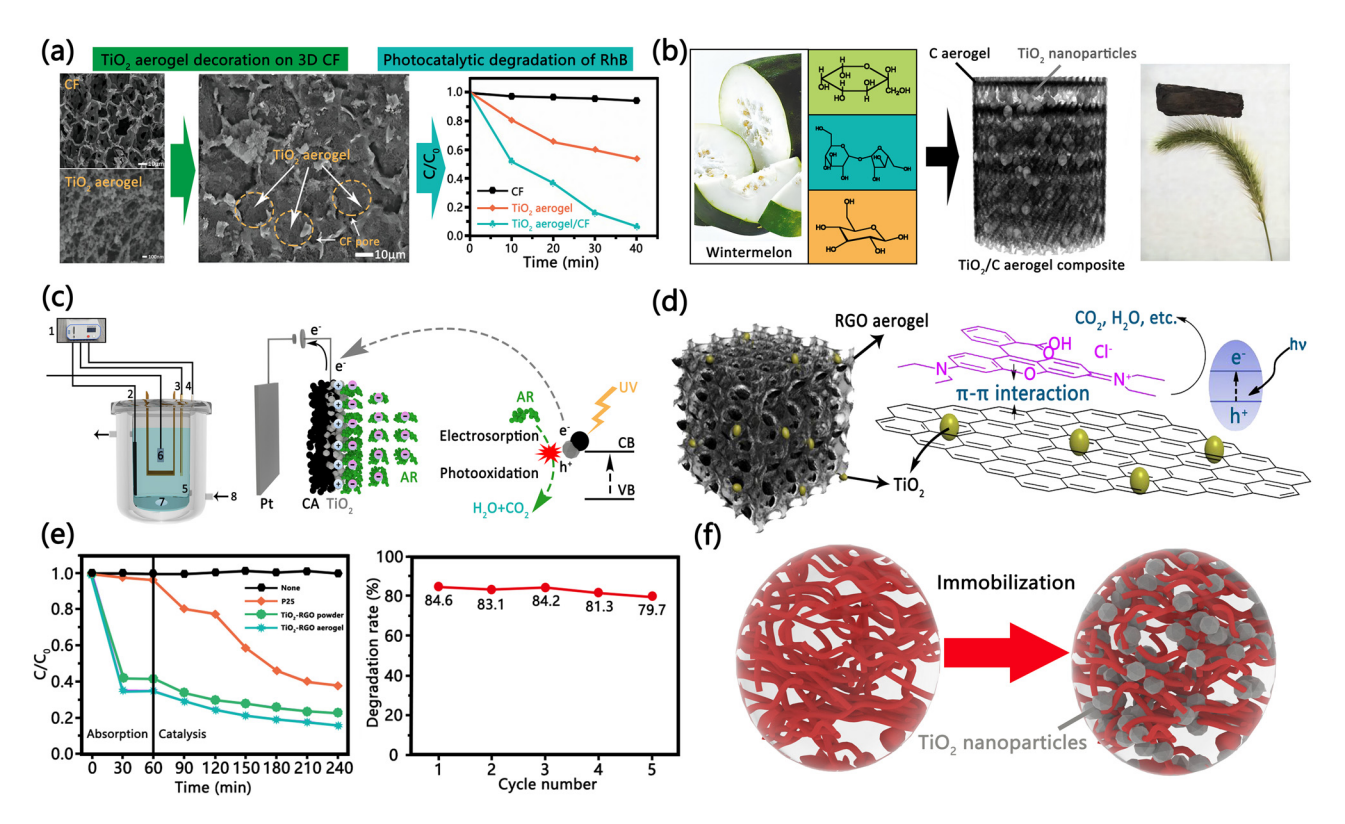


Figure 8: (a) SEM images and photocatalytic degradation curve of rhodamine B solution of the C foam, the TiO_2 aerogel, and the TiO_2 aerogel/C foam composite; (b) active functional groups in the framework of C aerogels synthesized from wintermelon, which are beneficial to the fixation and growth of TiO_2 nanoparticles, and the demonstration of the ultra-low density of the composite aerogel; (c) schematic diagram of the photocatalysis-enhanced electrosorption reactor (1-electrochemical workstation, 2- TiO_2 /C aerogel, 3-saturated calomel electrode, 4-counter electrode, 5-quartz tubular, 6-UV lamp, 7-magnetic stirring, and 8-circulating water), and the mechanism of the photocatalysis-enhanced electrosorption process on the TiO_2 /C aerogel; (d) schematic illustration of the selective adsorption and photodegradation mechanism of TiO_2 -RGO aerogels; (e) adsorption and photocatalytic degradation curves of the P25, the TiO_2 -RGO powder and the TiO_2 -RGO aerogel on rhodamine B solution, and relationship between the catalytic efficiency of the TiO_2 -RGO aerogel and the number of times of use; and (f) schematic illustration of the immobilization of TiO_2 nanoparticles in the regenerated cellulose matrix. (a) Modified with permission from ref. [102]. Copyright 2019, Elsevier. (b) Modified with permission from ref. [65]. Copyright 2016, Royal Society of Chemistry. (d) and (e) Reproduced with permission from ref. [105]. Copyright 2020, Elsevier.

pure TiO_2 aerogel and 20% of the Degussa-P25 under the same conditions [65].

Generally, in high-concentration dye sewage, photocatalysts are prone to deactivation due to the adsorption of dye molecules, which makes the surface unable to accept light excitation, while the photocatalysis-enhanced electrosorption process that can be achieved by TiO₂/C composite aerogels can solve this problem well [32]. Under the action of electrochemical polarization, the dye molecules can be enriched on the C electrode, and TiO₂ aerogels on the C electrode can degrade the dye molecules, thereby releasing the adsorption sites to carry out the process continuously. Meanwhile, the adsorption makes the dye molecules on the surface of TiO₂ aerogels always in a suitable concentration, which ensures the high efficiency of the photocatalytic reaction. Also, generating a positive voltage on TiO₂ aerogels can effectively separate photogenerated

electrons into an external circuit, improving the separation efficiency of electron—hole pairs. Under 0.6 V external voltage and 80 W UV light irradiation, the ${\rm TiO_2/C}$ composite aerogel electrode (effective working area 3.6 cm²) produced a maximum degradation efficiency of 97.3% (240 min) for 3,4-dihydroxy-9,10-dioxo-2-anthracenesulfonic acid sodium salt solution (400 mg/L, 80 mL), which was 3.1 times that of the electrochemical adsorption process, and successfully realized the efficient treatment of high-concentration dye sewage (Figure 8(c)).

In addition, the composite of graphene and TiO_2 aerogels has also become one of the research hotspots in recent years. Graphene has a specific surface area (up to $4,000 \,\text{m}^2/\text{g}$) far exceeding that of TiO_2 aerogels and a huge potential adsorption capacity for pollutants, and the formation of the TiO_2 –graphene aerogel composites' structure can better utilize this property, especially

for the pollutants with aromatic structures, such as methylene blue, rhodamine B, etc., which can form a π - π stacking effect with the aromatic regions of graphene sheets, so that they can be adsorbed on graphene sheets very efficiently and selectively [104]. Also, graphene is an excellent electron acceptor due to its π -conjugation structure, which can effectively inhibit the recombination of electron-hole pairs. The 2-dimensional planar structure of the graphene also has ultra-high electrical conductivity, so that photogenerated electrons can be easily transferred to the reaction sites (Figure 8(d)) [105]. Therefore, the graphene, especially the graphene aerogel, has become an ideal material to form composite aerogels with TiO2. In a dark environment, the one-pot self-assembled TiO₂–graphene aerogel composite (5 mg) achieved the highest adsorption rate of 95.1% (180 min) for rhodamine B solution (20 mg/L, 50 mL), and under the irradiation of 300 W pulsed tritium lamp, it achieved the highest photocatalytic degradation rate of 98.7% (180 min) [33]. In a dark environment, the hydrothermally synthesized TiO2-RGO hybrid aerogel (40 mg) yielded a 65.3% adsorption efficiency for highconcentration rhodamine B solution (1 g/L, 100 mL). Under the subsequent 180 min irradiation of 150 W tritium lamp, it achieved the highest degradation rate of 84.6%. Meanwhile, the composite aerogel also exhibited excellent recyclability, still yielding a high efficient photocatalytic degradation rate of up to 79.7% at the fifth use (Figure 8(e)) [105].

In addition, cellulose aerogels not only possess the excellent properties of high tensile strength, high crystallinity, and good biocompatibility of cellulose fibers, but also form a 3-dimensional and uniformly sized nanoporous structure, so they have been studied as a catalyst carrier for TiO₂ nanomaterials (Figure 8(f)) [106]. Under the irradiation of 254 nm UV lamp, the degradation rate of methyl orange dye (10 mg/L, 150 mL) by the spherical TiO₂ aerogel composite (50 mg) synthesized by cellulose alcohol-gel method was as high as 92.9% (90 min) [107]. Under the irradiation of ultraviolet light, the TiO₂-cellulose composite aerogel regenerated by dissolving cellulose with ionic liquid produced about 85% degradation rate for rhodamine B solution [108].

Organic photosensitization is another important means to improve the photocatalytic properties of TiO_2 aerogels [109]. Most organic sensitizers have a large π -ring conjugated delocalized system, a wide visible light response range, and super electron donating ability, which can be effectively controlled by modifying their molecular structure. In addition, due to the special nanoporous structure of TiO_2 aerogels, the different modes of action of the organic sensitizers will also lead to different improvements

achieved. Under the irradiation of 350 W tritium lamp and the acidic atmosphere created by 40 μ mol/L formic acid, the red cabbage anthocyanins as structure-directing agents embedded TiO₂ aerogel composite (50 mg) achieved a maximum degradation rate of 98% (30 min) for Cr⁶⁺ (15 ppm, 50 mL) that could not react with pure TiO₂ aerogels, and the effect achieved was more than twice that of the TiO₂ aerogel obtained by the surface adsorption of red cabbage anthocyanins [110].

In order to realize the multifunctional application of TiO₂ aerogels, environmentally friendly sodium alginate has also been studied as their catalyst carrier. The multifunctional TiO2-alginic acid composite aerogel synthesized by ion-crosslinking and freeze-drying has abundant -OHs and nanoscale rough skeleton surface, which ensures the realization of underwater oil-water separation function. The composite aerogel exhibited the highest oil-water separation efficiency of 99.7%, and had good oil-fouling resistance (the oleophobic angles for kerosene and pump oil were as high as 140.2° and 145.7°, respectively), and its repeated use rate in water was at least 60 times (99.2%). Under the irradiation of 300 W tritium lamp, it (35 mg) produced a maximum degradation rate of 97.6% (150 min) for methylene blue solution (10 ppm, 100 mL), and still reached 87.0% (150 min) in the sixth use, thus also showing good reusability in terms of photocatalytic properties [31]. In addition, the photocatalytic effects achieved by TiO₂ aerogels doped or composited with non-metallic substances are shown in Table 3.

5 TiO₂ aerogel composite photocatalysts for hydrogen energy production

5.1 Mechanism of photocatalysis

Since 1972, Fujishima and Honda [6] of the University of Tokyo discovered the new phenomenon of photocatalytic decomposition of water on ${\rm TiO_2}$ single crystal electrode to produce hydrogen, revealed the possibility of direct decomposition of water by solar energy, and opened up the research road for photo-splitting water using solar energy, the research on the synthesis of nanoscale photocatalysts for the photolysis of water to realize the rapid and efficient production of hydrogen has gradually attracted attention, and has achieved breakthrough progress in recent years.

Fable 3: Summary of degradation effects of TiO₂ aerogels doped or compounded by non-metallic substances on various environmental pollutants

Catalysts	Usage amount	Condition	Target	Time (min)	Time (min) Removal efficiency (%) Ref.	Ref.
${ m TiO}_2$ -C hybrid aerogel	50 mg	500 W UV light	Methylene blue (20 ppm, 50 mL)	180	96.6	[30]
TA/C foam composite	1.0 g/L	100 mW/m² sunlight	Rhodamine B $(1 imes 10^{-5} ext{mol/L})$	40	100	[102]
TiO ₂ /C aerogel composite	10 mg	500 W tungsten lamp	Methylene blue (40 mL, 40 mg/L)	210	82	[65]
${ m TiO_2/C}$ composite aerogel electrode	Working area 3.6 cm²	0.6 V external voltage and 80 W UV light	AR (80 mL, 400 mg/L)	240	97.3	[32]
TiO ₂ -graphene aerogel composite	5 mg	300 W tritium lamp	Rhodamine B (50 mL, 20 mg/L)	180	7.86	[33]
TiO ₂ –RGO hybrid aerogel	40 mg	150 W tritium lamp	Rhodamine B (100 mL, 1,000 mg/L)	180	84.6	[105]
Spherical TiO ₂ aerogel	50 mg	254 nm UV lamp	Methyl orange (150 mL, 10 mg/L)	90	92.9	[107]
RCA inserted TA nanocomposite	50 mg	350 W tritium lamp	Cr ⁶⁺ (50 mL, 15 ppm)	30	86	[110]
TiO ₂ -alginate composite aerogel	35 mg	300 W tritium lamp	Methylene blue (100 mL, 10 ppm)	150	9.76	[31]
Prussian blue modified SiO ₂ –TiO ₂	35 mg	150 W Xe/Hg lamp	Cr ⁶⁺ (35 mL, 20 mg/L)	09	66	[20]
aerogel Tungstate doped TiO ₂ –SiO ₂ aerogel	20 mg	350 W Xe lamp	Methamphetamine (50 mg/L, 50 mL) 60	09	98.8	[111]

Note: AR is the 3,4-Dihydroxy-9,10-dioxo-2-anthracenesulfonic acid sodium salt.

In the field, nano-TiO2 has attracted much attention because its conduction band potential is slightly negative than the hydrogen electrode potential $E(H^+/H_2)$, while the valence band potential is lower than the oxygen electrode potential $E(O_2/H_2O)$, and also has the advantages of high stability, no light corrosion, low cost, can absorb sunlight, and can meet the thermodynamic requirements of water splitting [112,113]. The structural features of aerogels, such as large specific surface area, high porosity, the 3-dimensional interconnected nanoscale framework, etc., are well suited for mass transfer applications, which are undoubtedly beneficial to further improve the photocatalytic hydrogen production rate. Therefore, under the same conditions, the hydrogen production rate of TiO2 aerogels is theoretically much higher than that of other types of TiO₂ nanomaterials.

Meanwhile, the intrinsic mechanism of the photocatalytic water splitting for hydrogen production is relatively consistent with the photocatalytic degradation of pollutants [114-117]. When the photon energy absorbed by TiO₂ aerogels is greater than the bandgap, electron hole pairs can be excited, and then the uncombined electrons and holes participate in different redox reactions to achieve the purpose of hydrogen production, as shown in equations (14)–(17) (Figure 9(a)). Also, it should be emphasized that photocatalytic reactions can be divided into energy barrier lowering reactions and energy barrier raising reactions [118,119]. O_2^- , OH^- , etc., generated by consuming holes in the energy barrier lowering reaction of the photocatalytic degradation of organic matters can be used as electron donors in the energy barrier raising reaction of the photocatalytic water splitting, which can significantly increase the hydrogen production rate and accelerate the transition from low-energy-density solar energy to high-energy-density hydrogen energy. Therefore, the combination of organic matters and water is almost always used as the object of photocatalysis, and the photocatalytic hydrogen production curves can be divided into the following three stages: (1) the rising stage, corresponding to the time required for H2 to be detected, (2) the peak stage, corresponding to the maximum H2 production rate under the experimental conditions, and (3) the descending stage, corresponding to a decrease in the rate of H₂ production due to the depletion of organic matters (Figure 9(b)) [120].

$$2hv \to 2e^- + 2h^+,$$
 (14)

$$2h^+ + H_2O \rightarrow 1/2O_2 + 2H^+,$$
 (15)

$$2H^{+} + 2e^{-} \rightarrow H_{2},$$
 (16)

$$2hv + H_2O \rightarrow 1/2O_2 + H_2$$
. (17)

5.2 Modification of TiO₂ aerogels for photocatalytic H₂ production

The research on the photocatalytic water splitting of TiO₂ aerogels for hydrogen production started late. As early as 2011, the effect of the structural advantages of aerogels on the photocatalytic hydrogen production rate was systematically investigated. The three-dimensional porous nanoscale network structure of TiO2 aerogels can diffuselv reflect incident light waves to the millimeter scale. thereby increasing the absorption efficiency of light. In addition, their ultra-high porosity helps to facilitate the delocalization of charge carriers to improve the separation of electron-hole pairs, and also greatly improves the kinetics of H₂ generation due to improved mass transfer processes for water, organics, etc. For instance, although the specific surface area of the TiO_2 aerogel (84.6 m²/g) was lower than that of the hydrothermally synthesized TiO_2 nanocrystal (115.7 m²/g), its H₂ production rate was 3.40 times that of the latter under the same conditions, and 9.63 times that of the Degussa-P25 under the same conditions [121].

Pt nanoparticles are often used as cocatalysts, which can not only improve the photocatalytic properties of TiO₂

aerogels through the LSPR, but also have a more positive Fermi level than TiO₂, thus attracting and capturing electrons to further promote the generation of H₂ [122]. Generally, the modification of TiO2 aerogels by Pt nanoparticles with suitable particle size and mass fraction can increase the hydrogen production rate by at least one order of magnitude. Under the irradiation of 400 W mercury lamp and the temperature of 20°C, the 1.9 nm Pt nanoparticles (0.05 wt%) surface-modified TiO₂ aerogel (0.1 g) synthesized by the impregnation-calcination-reduction process and the 4.7 nm Pt nanoparticles (0.5 wt%) surface-modified TiO₂ aerogel (0.1 g) synthesized by the polyol process produced nearly equal H2 production rates to methanol solution (50 vol%, 50 mL), both of which were about 290 µmol/(g h), which was much higher than 18.3 µmol/(g h) of the pure TiO₂ aerogel under the same conditions [121]. Thereinto, smaller Pt nanoparticles mean wider spatial distribution, resulting in more photocatalyst-cocatalyst binding sites, that is, more reaction sites, so they can achieve hydrogen production rates comparable to larger Pt nanoparticles at a lower loading.

Subsequent studies provided a more detailed explanation of the effect of the particle size of the doped Pt nanoparticles. When the particle size of Pt nanoparticles

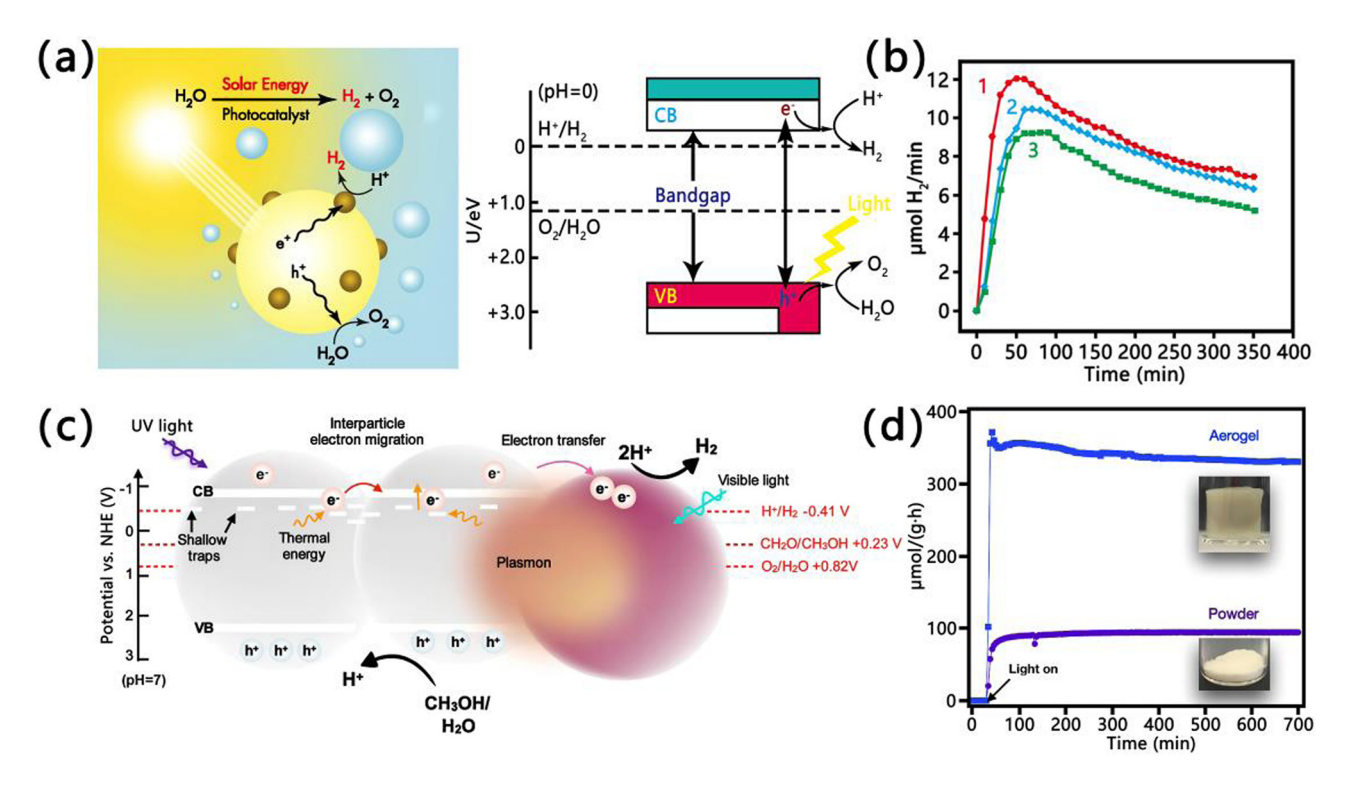


Figure 9: (a) Schematic diagram of macroscopic and microscopic mechanisms of the photocatalytic hydrogen production from TiO_2 aerogels; (b) evolution of H2 by ethanol photocatalytic reforming in the presence of TiO_2 -Pt composite aerogel with various Pt sizes: (1) 5.75 nm; (2) 6 nm; and (3) 6.5 nm. The photodegradable solution contained 1% ethanol; (c) representation of the electron migration process in the aerogel network; and (d) H_2 evolution using Pd- TiO_2 aerogels and their respective powders. (b) Modified with permission from ref. [120]. Copyright 2014, Elsevier. (c) and (d) Reproduced with permission from ref. [18]. Copyright 2020, Elsevier.

is less than 1 nm, the quantum size effect makes the working function very high, while the working function of bulk Pt or Pt nanoparticles with larger particle size is about -5.65 eV, and the corresponding levels of the valence band and the conduction band of TiO2 nanocrystals are about -7.6 and -4.4 eV, respectively [123]. That is to say, when the particle size of Pt nanoparticles is sufficiently small, no injection of electrons can take place since the metal then lies too high. When the particle size of Pt nanoparticles is large, in addition to the injection of electrons, holes can also be injected from the valence band of TiO₂ to the nearest metal energy state, which accelerates the recombination of electron-hole pairs [124,125]. Therefore, only moderately small Pt nanoparticles are suitable for the modification of TiO2 aerogels. Up to now, the photocatalytic hydrogen production rate of Pt nanoparticles doped TiO2 aerogels is already comparable to the highest hydrogen production levels reported for other types of nanomaterials. Under the irradiation of 400 W UV lamp, the photocatalytic hydrogen production rate of the 5.75 nm Pt nanoparticles (1 wt%) doped TiO₂ aerogel (0.1 g) for water containing 1 vol% of ethanol (100 mL) was up to $7,200 \, \mu \text{mol/(g h)}$ [120].

Based on the doping of Pt nanoparticles, the doping of N atoms can not only broaden the absorption spectrum of ${\rm TiO_2}$ aerogels, but also form a synergistic effect with Pt nanoparticles, responsible for increasing the photocatalytic activity and the hydrogen production rate. Under the irradiation of 250 W high pressure mercury lamp, the hydrogen production rate of the N (1 at%)/Pt-TiO₂ aerogel for salicylic acid solution (5 \times 10⁻⁴ mol/L) was 1.2 times that of the sample without doping N atoms under the same conditions [126].

The LSPR of Au nanoparticles can span a large part of the visible spectrum and become yet another metal dopant for the visible light-driven photocatalytic water splitting of TiO₂ aerogels for hydrogen production. DeSario et al. [127] reached the same conclusion as previously mentioned Pennington et al. [96] on the influence of doping methods of Au nanoparticles on the structures of TiO₂ aerogels. That is, the surface modification of Au nanoparticles usually weakens the structural characteristics of TiO2 aerogels, and is prone to surface migration and agglomeration, which weakens the strength of the LSPR. While the uniform doping of Au nanoparticles can overcome these problems well. On the effect of doping methods on the photocatalytic properties, DeSario et al. made a more indepth study. Compared with the surface modification of Au nanoparticles, the TiO₂ aerogel uniformly doped by Au nanoparticles produces a higher incident photon-electron conversion efficiency, a higher photovoltage value, a shorter steady-state photovoltage generation time, and

a faster excited-state electron reaction in any wavelength band of the photoaction spectra, which is mainly related to the uniform doping of Au nanoparticles resulting in more photochemical reaction interphases and a higher plasmonic-to- TiO_2 charge carrier conversion efficiency.

Meanwhile, it should be emphasized that for the doping of metal nanoparticles, the nanoparticles selfassembly synthesis is a more suitable method to prepare TiO₂ aerogels than the sol-gel method. As mentioned earlier, the nanoparticle self-assembly can directly synthesize highly crystalline TiO₂ aerogels without high-temperature crystallization, so they have more prominent aerogels' structural properties. More importantly, the directional attachment during self-assembly of crystallized TiO2 nanoparticles creates edge defects due to tiny dislocations at the interface, which are closely related to the formation of shallow traps. Specifically, shallow traps are energies located below the conduction band of TiO2 and the distance between the two is less than the thermal energy of electrons (0.26 eV at 300 K). As a result, the electrons in shallow traps can be excited into the conduction band of TiO2, or trapped in another shallow trap and then excited into the conduction band of TiO2, which is beneficial to the generation of H₂, as shown in Figure 9(c) [18]. Taking the doping of Au nanoparticles as an example, the nanoparticles self-assembly synthetic TiO₂ aerogels can form a light wave absorption of about 400-500 nm, which has a large overlap with the LSPR of Au nanoparticles, and the formed combination is conducive to the formation of H2 by the near-field electromagnetic mechanism. Also, the LSPR of Au nanoparticles is beneficial to accelerate the migration of shallow traps and further promote the generation of H₂.

In addition, the nanoparticles self-assembly synthetic TiO₂ aerogels also have good long-term application stability. Taking the photocatalytic study of the nanoparticles self-assembly synthetic Pd nanoparticles doped TiO₂ aerogel for methanol aqueous solution (50 vol%) as an example [18]. At the beginning of the reaction, the H₂ generation rate fluctuated significantly, which was mainly related to the degradation of the organic matter as the directing agent in the self-assembly synthesis, which interfered with the photocatalytic reaction. Subsequently, the H₂ generation rate remained relatively stable for a long time. Meanwhile, the aerogel was ground into powder to only change the porosity without changing other structural characteristics, the long-term stable hydrogen production rate that can be obtained was only about 2/7 of the bulk form, which also demonstrated the importance of the 3-dimensional interconnected nanoporous structure of aerogels for photocatalytic reactions (Figure 9(d)).

To sum up, although ${\rm TiO_2}$ aerogel composites have less research on the photocatalytic water splitting for hydrogen production and have not formed a complete research system, from the results of the research, they are extremely promising in this application road. Recently, it has been reported that black ${\rm TiO_2}$ consisting of approximately 2 nm of thin disorder layer around the surface showed surprisingly high solar hydrogen generation ability, which may be one of the milestones for the future breakthrough in the photocatalytic hydrogen production rate of ${\rm TiO_2}$ aerogels [128].

6 Analysis and discussion on the future development of TiO₂ aerogels

6.1 Research direction – structural engineering design

Up to now, most of the research focused on the synthesis techniques and the photocatalytic properties' improvement

of ${\rm TiO_2}$ aerogels, and only a few reports used other nanomaterials such as C nanomaterials, nanocellulose matrix, *etc.*, to improve their mechanical properties, but this does not fundamentally overcome the problem. With the rapid development of the aerogels' field in recent years, the structural engineering design not only gives a clear definition on the classification of aerogels [129], which defines aerogels composed of nanoparticles, nanofibers, and nanosheets as basic elements as 0D granular, 1D fibrous, and 2D laminar aerogels (Figure 10(a)) [37,130,131], respectively, but also provides a new option for overcoming the weak mechanical properties of ${\rm TiO_2}$ aerogels.

Structural engineering design considers porosity, pore size, and the ratio of relative Young's modulus ($E/E_{\rm s}$) to relative density ($\rho/\rho_{\rm s}$) as the reasons for the differences in the mechanical properties of aerogels [129]. The porosity of 0D granular aerogels is often below 90%, the pore size is distributed at the nanoscale and the relative density is high, while the porosity of 1D fibrous and 2D laminar aerogels is often above 99%, the pore size is distributed at the micrometer scale and the relative density is low. Generally, the larger the porosity and pore size distribution, the larger the deformation space and degree of freedom, which can adapt to the deformation behavior of the basic elements of

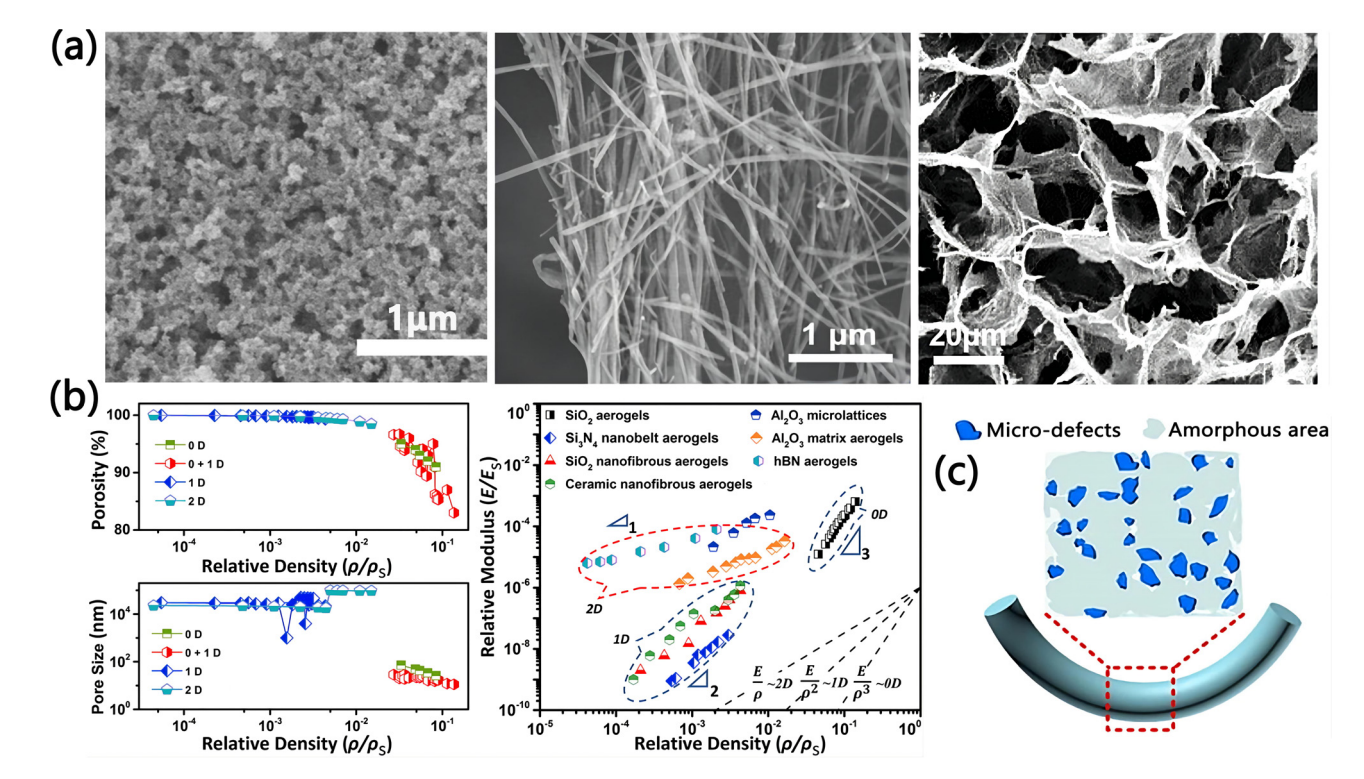


Figure 10: (a) SEM images of representative 0D granular, 1D fibrous, and 2D laminar aerogels; (b) the porosity, pore size, and elastic deformability of 0D granular, 1D fibrous, and 2D laminar aerogels; and (c) schematic of the microstructure of a bent SiO₂ nanofiber. (a) Reproduced with permission from ref. [37]. Copyright 2020, Elsevier; Reproduced with permission from ref. [130]. Copyright 2020, American Association for the Advancement of Science; Reproduced with permission from ref. [131]. Copyright 2019, American Association for the Advancement of Science. (b) Reproduced with permission from ref. [129]. Copyright 2020, Elsevier. (c) Reproduced with permission from ref. [133]. Copyright 2018, American Association for the Advancement of Science.

aerogels, resulting in the generation of flexibility and elasticity. Also, the $E/E_{\rm s}$ of OD granular aerogels is proportional to the $(\rho/\rho_{\rm s})^3$, which meets the condition that the mechanical properties are rigid and brittle, while the $E/E_{\rm s}$ and the $(\rho/\rho_{\rm s})^{1-2}$ of 1D fibrous and 2D laminar aerogels have a linear relationship. It is precisely because of the decrease in the ratio of the $E/E_{\rm s}$ and the $\rho/\rho_{\rm s}$ that the elastic deformation capacity is generated. The specific investigation results are shown in Figure 10(b).

From a structural point of view, the mechanical properties of the OD granular aerogels' framework are supported by the weak neck region formed between the secondary particles, and this weak and rigid connection is the root cause of the weak mechanical properties [132]. Compared with 0D granular aerogels, 1D fibrous aerogels can effectively eliminate the point-to-point cross-linking mode to form a continuum structure, which enhances the tensile and bending properties, while enhancing the compressive properties [130]. Generally speaking, the necessary condition for 1D fibrous aerogels to produce high flexibility is that both the nanofibers and the crosslinked components are amorphous, so that the resulting dispersed defects act as lubricating regions, which can effectively disperse external stress to generate large deformations, such as glassy SiO₂ nanofibers can achieve this effect (Figure 10(c)) [133]. However, TiO₂ aerogels can only have photocatalytic properties under the condition of crystallization, and it is obviously impossible to realize the formation of TiO2 fibrous aerogels only with crystallized TiO₂ nanofibers. According to the synthesis experience of other nanofibrous aerogels, at least the following ideas can be used for reference. The monolithic encapsulation of crystallized TiO2 nanofibers can be formed by an amorphous and optically transparent cross-linking component, resulting in a continuous core-shell structure, which not only ensures the formation of TiO₂ fibrous aerogels, but also does not affect the absorption of light waves, so as to achieve their excellent photocatalytic properties. The reported fibrous aerogel with SiO2 as the shell and SiC nanowires as the core fully demonstrates the feasibility of this idea (Figure 11(a) and (b)), which exhibits not only excellent recoverable radial compression (recovery after 80% compressive strain) but also excellent fatigue resistance (Figure 11(c)) [130]. In addition, using a variety of nanofibers as a support and cross-linking matrix for 0D granular TiO2 aerogels is also a simple technique to improve the mechanical properties. Nanofibers can form a layered network and form interfacial bonds with TiO₂ nanoparticles through in situ cross-linking, thereby endowing TiO₂ aerogels with the ability to elastically deform. There are many precedent studies on this idea in SiO₂ aerogels.

Compared with the compressive strain of pure SiO_2 aerogels of less than 10%, the elastic deformation ability and fracture resistance of nanofiber-reinforced SiO_2 aerogels are significantly improved, and the current research has achieved a fracture strain over 80% with an ultimate stress up to 7.3 MPa (Figure 11(d)) [134].

Compared with 0D granular and 1D fibrous aerogels, 2D laminar aerogels exhibit stronger elastic deformation ability. The reported h-BN aerogel with hyperbolic macrostructure and double-pane wall substructure exhibits 95% compression deformation, which is mainly due to the nano-hierarchical flexibility of cell walls and the negative exponential meta-structural design (Figure 11(e)) [131]. In 2D laminar aerogels' structures, nanosheets are easily deformed due to their extremely high aspect ratio, and are separated from each other to withstand forces. The strong face-to-face cell walls act as the basic elastic unit, capable of restoring themselves to their original shape under a wide range of deformations, which is mainly related to the face-to-face stacking of 2D nanosheets, optimizing the load transfer path and enhancing the frame stiffness of cell walls. Based on this advanced concept, the construction of 2D laminar TiO2 aerogels' systems with excellent mechanical properties is likely to be a hot research direction in the future.

6.2 Application direction – exploration of industrialization road

The meaning of the birth of a functional material is to mass-produce it for application after the production technique becomes mature, so as to create greater value for the society, and TiO₂ aerogels are also the same. According to the research status, the biggest obstacle in realizing the large-scale production and application of TiO₂ aerogels is the lack of a mature production technique, because it is related to factors such as production cost, production cycle, products' performance, environmental protection, etc., that need to be considered. Nowadays, the sol-gel method in which TiO2 aerogels are obtained by hydrolysis and polycondensation to form TiO2 wet gels followed by supercritical drying or ambient pressure drying is still the preferred technique for preparation. However, the TiO₂ aerogels obtained by sol-gel are amorphous, and cannot be directly applied. The application scale of the supercritical drying is small, and it also has the disadvantages of complicated operation and high energy consumption. The ambient pressure drying consumes a lot of organic reagents, which is easy to cause environmental pollution,

24 — Xin Long et al. DE GRUYTER

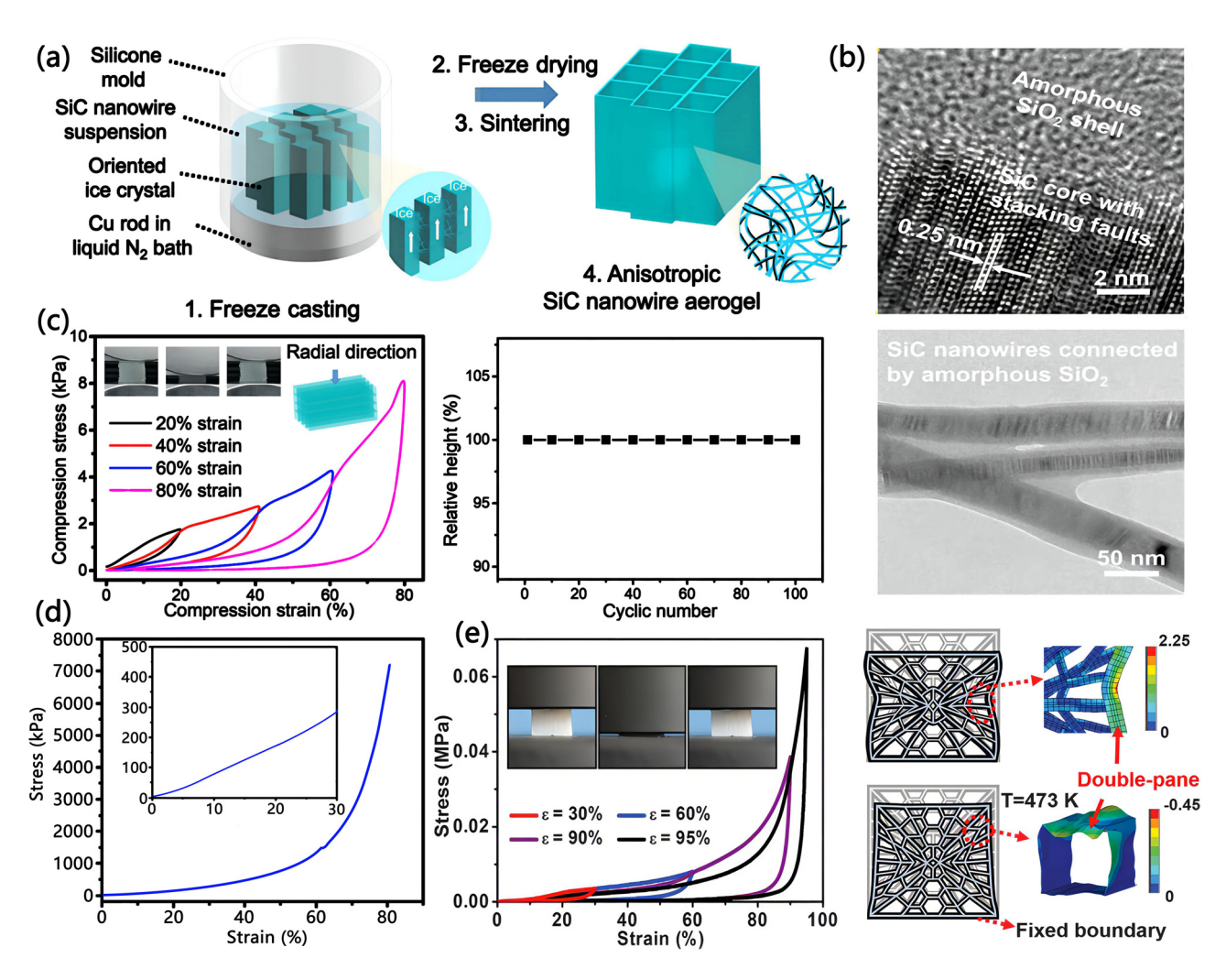


Figure 11: (a) Fabrication process of the anisotropic and hierarchical SiC@SiO₂ nanowire aerogel; (b) high-resolution TEM image of the SiC@SiO₂ nanowire; (c) compression stress–strain curve of the SiC@SiO₂ nanowire aerogel in the radial direction, and the relative height evolution during 100 compression cycles; (d) stress–strain curve of the chitosan-SiO₂ aerogels under compression; (e) uniaxial compression of hexagonal boron nitride aerogels with repeatable strain up to 95%, and illustration of the metastructure design of the hexagonal boron nitride aerogel. (a)–(c) Reproduced with permission from ref. [130]. Copyright 2020, American Association for the Advancement of Science. (d) Modified with permission from ref. [134]. Copyright 2019, American Association for the Advancement of Science.

and the cycle is relatively long. These limitations have hindered the most widely used technique as a means of realizing the industrialization of ${\rm TiO_2}$ aerogels, as mentioned before.

If the drying process can be carried out simultaneously as the sol–gel reaction, there is no doubt that the preparation cycle can be shortened by orders of magnitude, and all the disadvantages related to time will be reduced. Following this concept for the production of ${\rm TiO_2}$ aerogels is undoubtedly in line with their industrialization development path. Throughout the preparation process in the entire aerogels' field, only the rapid supercritical extraction (RSCE) technique, which was born

nearly 15 years ago and has not been paid attention to at all, is expected to achieve the above goal [135]. Instead of autoclaves or pressure vessels, the RSCE often uses hydraulic heat presses to heat and close the molds, which is currently the only method that can realize aerogel in one step. Thereinto, Union RSCE is slightly more common (Figure 12(a)) [136]. After the liquid mixture of aerogel precursors is poured into a metal mold, the mold is sandwiched between a kapton film and a high temperature gasket and placed in a hot press. At the beginning of the reaction, the hot press is closed to seal the mixture in the mold, and it continuously provides a compression-inhibiting force. During the gradual heating process, the

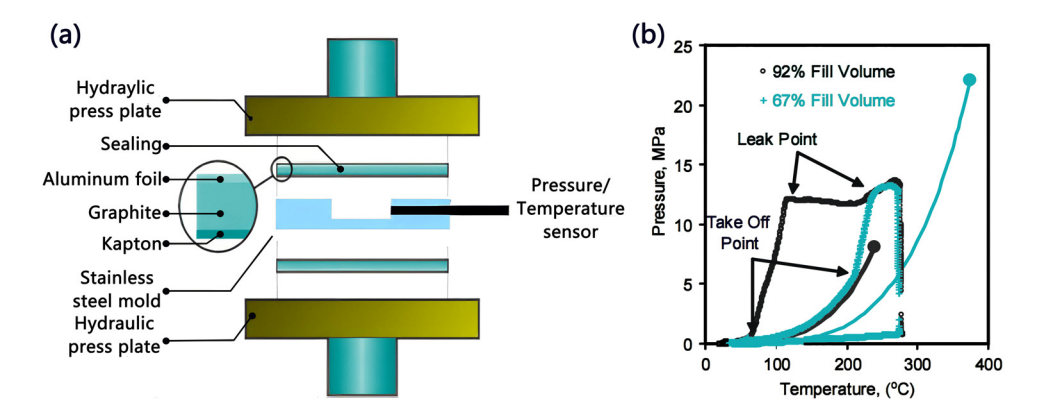


Figure 12: (a) Schematic of hot press platens and aerogel mold (not to scale). The mold is instrumented with a pressure and temperature sensor and sealed using a graphite/Kapton gasket. Aluminum foil is used to prevent the gasket material from sticking to the platens; (b) the pressure and temperature in the mold were measured during RSCE processing using a melt transducer. Pressure and temperature data shows the takeoff and leak points for two different initial fill volumes. (a) and (b) Modified with permission from ref. [136]. Copyright 2009, Elsevier.

aerogel precursors begin to react to form wet gels with nanoporous structures. The pressure throughout the process is a function of the temperature system and cannot be controlled directly, and there is a take-off point and a leak point (Figure 12(b)). The take-off point refers to the starting position of the pressure surge in the closed mold, which is related to the volume ratio of the liquid mixture and is mainly caused by the volume expansion and phase transition of the solvents during the heating process. The leak is determined as a function of the mechanical force acting on the system. When the pressure value in the mold is close to that of the hot press gasket, leakage will occur, and the pressure value of the gasket can be adjusted flexibly. Therefore, when the solvents reach the supercritical state and the pressure in the mold reaches the pressure value of the gasket, the supercritical fluid formed is gradually released and the pressure gradually drops, leaving the aerogel behind. In the precedent study, the technique achieved the preparation of SiO₂ aerogels in one step within 3 h, which fully demonstrated the feasibility and practicability.

In addition to the ultra-short preparation cycle, the RSCE technique has other advantages for the preparation of TiO₂ aerogels. The aerogels' framework is formed under high temperature and high pressure during the synthesis of the RSCE. Thus, expensive organic Ti alkoxides such as titanium tetrabutoxide, isopropyl titanate, *etc.*, are no longer applicable due to their extremely high reactivity with water, making it difficult to carry out controllable reactions. While inorganic titanium salt precursors such as TiCl₄ can just have suitable reactivity with water under the energy supply of high temperature and high pressure, which is very beneficial to the formation of high-quality TiO₂ aerogels' framework and directly reduces

the cost of raw materials. In addition, short-term high-temperature treatment is helpful for the pre-crystallization process of TiO₂ aerogels, which not only makes the newly made TiO₂ aerogels have certain photocatalytic properties, but also makes reasonable use of high-temperature energy in the synthesis process. Also, the acid anions in inorganic titanium salt precursors remaining on the surface of TiO₂ aerogels can also play a role in separating electron—hole pairs to a certain extent.

In summary, the RSCE not only has the ability to quickly and efficiently produce ${\rm TiO_2}$ aerogels within a few hours, but also forms a good fit with the synthesis of ${\rm TiO_2}$ aerogels. Therefore, the RSCE technique of ${\rm TiO_2}$ aerogels needs to be deeply studied in the future, and its maturity is enough to make the industrialization of ${\rm TiO_2}$ aerogels a big step forward.

7 Conclusion and outlook

As the first review report on TiO₂ aerogels and their composites, we provide a detailed review of the synthesis, properties, modifications, applications, and future prospects. Due to the structural characteristics of aerogels such as large specific surface area, high porosity, the 3-dimensional interconnected network structure composed of relatively uniform nanoparticles, high light transmittance, *etc.*, TiO₂ aerogels exhibit far superior photocatalytic properties than other TiO₂ nanomaterials, and also show better development prospects. Up to now, a total of three techniques have been developed for the preparation of TiO₂ aerogels. The sol–gel method has become the most widely used technique because of its simple process, low cost, ability to mix and react components on

an atomic scale, etc., but the newly made TiO_2 aerogels obtained from the sol–gel process are often amorphous and difficult to apply directly, and the subsequent high-temperature crystallization will lead to structural damage and energy loss. The nanoparticles self-assembly synthesis is proposed to overcome this problem, and the resulting products often have the structural characteristics of macroporous aerogels, with an ultra-high proportion of crystalline phases and multiple crystalline phases can coexist. The high-temperature aerosol technique adopts the idea of gas-phase synthesis to prepare highly crystalline and highly pure TiO_2 aerogels without any additives on the surface. In general, the three synthesis techniques have their own advantages and disadvantages, but they also show a space for integration and development that can complement each other's advantages.

In addition, according to the difference of the modification mechanism, we reasonably divide the modified substances into three categories: SiO₂ aerogels, metal dopants, and other non-metallic substances. The modification of SiO2 aerogels is mainly reflected in the more excellent structural characteristics of aerogels and can affect the recombination of photogenerated carriers and stabilize the anatase TiO2 to a certain extent. The modification of metal ions and metal nanoparticles is mainly reflected in the impact on the photocatalytic quantum process, such as reducing the bandgap, expanding the absorption range of light waves, inhibiting the recombination of photogenerated carriers, etc., and the focus of the two modifications is different. Also, they can also promote the formation of crystallized TiO₂ to some extent. The modification of non-metallic substances is relatively complicated, some of them can produce similar effects as metal dopants, and the rest depends on some intrinsic properties such as strong adsorption properties, oil-water separation function, electrocatalytic synergistic effect, etc., to further improve the photocatalytic properties of TiO₂ aerogels. In most literature reports on the environmental treatment, the modified TiO₂ aerogel composites can produce degradation rates of more than 90% within 120 min for simulated pollutants with different concentrations and different volumes. Although there are few reports on the hydrogen energy production, the photocatalytic hydrogen production rates achieved by the modified TiO₂ aerogel composites in these reports have been close to or comparable to the highest levels achieved by other types of nanomaterials, which indicates that they have good development prospects in this field.

Although a lot of research has been carried out and great progress has been made, there are still huge challenges in the research and application of TiO₂ aerogels. First, most studies focus on the improvement of the

photocatalytic properties of TiO₂ aerogels by using a single dopant or a composite component, and there are few reports on the joint improvement of multiple components. Also, the modification mechanism is not studied deeply enough to form a complete research system. Second, there are very few reports on overcoming the weak mechanical properties of TiO2 aerogels, which seriously hinders practical applications and limits the expansion of application directions. Therefore, there is an urgent need to strengthen research in this area in the future. Third, although several methods have been developed for the preparation of TiO₂ aerogels, none of them meet the requirements of large-scale industrial synthesis under the premise of low cost, high efficiency, and no environmental pollution. How to realize the industrialization of TiO2 aerogels like SiO2 aerogels is still a topic that needs to be explored for a long time. Thereinto, combined with the research status of TiO2 aerogels and the research experience of other types of aerogels, we put forward the solution ideas of the structural engineering design and the rapid supercritical synthesis on the research topics of improving the weak mechanical properties of TiO₂ aerogels and exploring the road to industrialization, respectively, and fully demonstrated the feasibility and rationality. Meanwhile, we also believe that these will be the future development directions of TiO2 aerogels. Although the road to continued development is long, the future of TiO₂ aerogels is promising with the deepening of the research.

Funding information: This work was supported by the Municipal Government of Quzhou under Grant Number 2021D006 the International Cooperation Projects of Sichuan Provincial Department of Science and Technology (2021YFH0126), the Fundamental Research Funds for the Central Universities (A030202063008029), the Natural Science Foundation of Shaanxi Province (2021JQ-538), and the China Postdoctoral Science Foundation (No. 2021T140433, 2020M683408).

Author contributions: All authors have accepted responsibility for the entire content of this manuscript and approved its submission.

Conflict of interest: The authors state no conflict of interest.

References

[1] Kim M, Kim YK, Lim SK, Kim S, In SI. Efficient visible lightinduced H₂ production by Au@CdS/TiO₂ nanofibers: **DE GRUYTER**

- Synergistic effect of core-shell structured Au@CdS and densely packed TiO_2 nanoparticles. Appl Catal B. 2015;166-167:423-31.
- [2] Noman MT, Ashraf MA, Ali A. Synthesis and applications of nano-TiO₂: a review. Environ Sci Pollut Res. 2018;26:3262-91.
- [3] Tesfamichael T, Will G, Bell J, Prince K, Dytlewski N.
 Characterization of a commercial dye-sensitised titania solar cell electrode. Sol Energy Mater Sol Cells. 2003;76:25–35.
- [4] Wang H, Liu X, Niu P, Wang S, Shi J, Li L. Porous twodimensional materials for photocatalytic and electrocatalytic applications. Matter. 2020;2:1377–413.
- [5] Xu T, Liu X, Wang S, Li L. Ferroelectric oxide nanocomposites with trimodal pore structure for high photocatalytic performance. Nano-Micro Lett. 2019;11:37.
- [6] Fujishima A, Honda K. Electrochemical photolysis of water at a semiconductor electrode. Nature. 1972;238:37–8.
- [7] Qiu B, Xing M, Zhang J. Mesoporous TiO₂ nanocrystals grown in situ on graphene aerogels for high photocatalysis and lithium-ion batteries. J Am Chem Soc. 2014;136:5852-5.
- [8] Lee K, Hahn R, Schmuki P. Photocatalytic H₂ production on self-decorated Au nanoparticles/TiO₂ nanotubes under visible light. Electrochem Commun. 2014;43:105–8.
- [9] Chatterjee D, Dasgupta S. Visible light induced photocatalytic degradation of organic pollutants. J Photoch Photobio C. 2005;6:186-205.
- [10] Montazer M, Pakdel E, Behzadnia A. Novel feature of nanotitanium dioxide on textiles: Antifelting and antibacterial wool. J Appl Polym Sci. 2011;121:3407-13.
- [11] Naldoni A, Altomare M, Zoppellaro G, Liu N, Kment S, Zbořil R, et al. Photocatalysis with reduced TiO₂: from black TiO₂ to co-catalyst-free hydrogen production. ACS Catal. 2019;9:345–64.
- [12] Watson JM, Cooper AT, Flora JRV. Nanoglued titanium dioxide aerogels for photocatalysis. Environ Eng Sci. 2005;22:666-75.
- [13] Moussaoui R, Elghniji K, Mosbah MB, Elaloui E, Moussaoui Y. Sol-gel synthesis of highly TiO_2 aerogel photocatalyst via high temperature supercritical drying. J Saudi Chem Soc. 2017:21:751-60.
- [14] Heiligtag FJ, Rossell MD, Süess MJ, Niederberger M. Template-free co-assembly of preformed Au and TiO₂ nano-particles into multicomponent 3D aerogels. J Mater Chem. 2011;21:16893.
- [15] Dilger S, Hintze C, Krumm M, Lizandara-Pueyo C, Deeb S, Proch S, et al. Gas phase synthesis of titania with aerogel character and its application as a support in oxidation catalysis. J Mater Chem. 2010;20:10032.
- [16] Alwin S, Shajan XS, Karuppasamy K, Warrier KGK. Microwave assisted synthesis of high surface area TiO₂ aerogels: A competent photoanode material for quasi-solid dye-sensitized solar cells. Mater Chem Phys. 2017;196:37–44.
- [17] Sui R, Rizkalla A, Charpentier PA. Experimental study on the morphology and porosity of TiO₂ aerogels synthesized in supercritical carbon dioxide. Micropor Mesopor Mater. 2011;142:688–95.
- [18] Luna AL, Matter F, Schreck M, Wohlwend J, Tervoort E, Colbeau-Justin C, et al. Monolithic metal-containing TiO₂ aerogels assembled from crystalline pre-formed

- nanoparticles as efficient photocatalysts for H_2 generation. Appl Catal B. 2020;267:118660.
- [19] Bernardes JC, Pinheiro GK, Muller D, Latocheski E, Domingos JB, Rambo CR. Novel modified nonalkoxide sol-gel synthesis of multiphase high surface area TiO₂ aerogels for photocatalysis. J Sol-Gel Sci Technol. 2020;94:425-34.
- [20] Zhu W, Yang H, Xie Y, Sun S, Guo X. Hierarchically porous titania xerogel monoliths: synthesis, characterization and electrochemical properties. Mater Res Bull. 2016;73:48-55.
- [21] Alwin S, Sahaya Shajan X, Menon R, Nabhiraj PY, Warrier KGK, Gowravaram MR, et al. Surface modification of titania aerogel films by oxygen plasma treatment for enhanced dye adsorption. Thin Solid Films. 2015:595:164-70.
- [22] Zhang BX, Yu H, Zhang Y, Luo Z, Han W, Qiu W, et al. Bacterial cellulose derived monolithic titania aerogel consisting of 3D reticulate titania nanofibers. Cellulose. 2018;25:7189-96.
- [23] Sadrieyeh S, Malekfar R. Photocatalytic performance of plasmonic Au/Ag-TiO₂ aerogel nanocomposites. J Non-Cryst Solids. 2018;489:33–9.
- [24] Zirakjou A, Aghdam RM, Soorbaghi FP. Synthesis and characterization of monolithic titania/nanoclay nanocomposite aerogels. Procedia Mater Sci. 2015;11:548-52.
- [25] Wei X, Cai H, Feng Q, Liu Z, Ma D, Chen K, et al. Synthesis of co-existing phases Sn-TiO₂ aerogel by ultrasonic-assisted sol-gel method without calcination. Mater Lett. 2018;228:379–83.
- [26] Zhao X, Ju W, Zhang J, Liu B, Zhang J, Yi X. Mesoporous TiO₂/ SiO₂/Ag ternary composite aerogels for high photocatalysis. New J Chem. 2019;43:6234–41.
- [27] Xu B, Ding J, Feng L, Ding Y, Ge F, Cai Z. Self-cleaning cotton fabrics via combination of photocatalytic TiO₂ and superhydrophobic SiO₂. Surf Coat Tech. 2015;262:70–6.
- [28] Long T, Xu Y, Lv X, Ran J, Yang S, Xu L. Fabrication of the annular photocatalytic reactor using large-sized free-standing titania-silica monolithic aerogel as the catalyst for degradation of glyphosate. Mater Design. 2018;159:195–200.
- [29] Wang C-T, Lai D-L. Synthesis and characterization of ironand vanadium-doped titania aerogel nanopowders. J Am Ceram Soc. 2011;94:2646–51.
- [30] Shao X, Lu W, Zhang R, Pan F. Enhanced photocatalytic activity of TiO₂-C hybrid aerogels for methylene blue degradation. Sci Rep. 2013;3:3018.
- [31] Dai J, Tian Q, Sun Q, Wei W, Zhuang J, Liu M, et al. TiO₂-alginate composite aerogels as novel oil/water separation and wastewater remediation filters. Composites Part B. 2019;160:480-7.
- [32] Jin Y, Wu M, Zhao G, Li M. Photocatalysis-enhanced electrosorption process for degradation of high-concentration dye wastewater on TiO₂/carbon aerogel. Chem Eng J. 2011;168:1248-55.
- [33] Zhang JJ, Wu YH, Mei JY, Zheng GP, Yan TT, Zheng XC, et al. Synergetic adsorption and photocatalytic degradation of pollutants over 3D TiO₂-graphene aerogel composites synthesized via a facile one-pot route. Photochem Photobiol Sci. 2016;15:1012–9.
- [34] Liu Y, Xiang Z. Fully conjugated covalent organic polymer with carbon-encapsulated Ni₂P for highly sustained

- photocatalytic H₂ production from seawater. ACS Appl Mater Inter. 2019:11:41313-20.
- [35] Moussaoui R, Elghniji K, Ben Mosbah M, Elaloui E, Moussaoui Y. Sol-gel synthesis of highly TiO2 aerogel photocatalyst via high temperature supercritical drying. J Saudi Chem Soc. 2017;21:751-60.
- Sung WJ, Hyun S-H, Kim D-H, Kim D-S, Ryu J. Fabrication of mesoporous titania aerogel film via supercritical drying. J Mater Sci. 2009;44:3997-4002.
- Yue X, Xiang J, Chen J, Li H, Qiu Y, Yu X. High surface area, high catalytic activity titanium dioxide aerogels prepared by solvothermal crystallization. J Mater Sci Technol. 2020;47:223-30.
- Shimoyama Y, Ogata Y, Ishibashi R, Iwai Y. Drying processes for preparation of titania aerogel using supercritical carbon dioxide. Chem Eng Res Des. 2010;88:1427-31.
- Sui R, Liu S, Lajoie GA, Charpentier PA. Preparing titania aerogel monolithic chromatography columns using supercritical carbon dioxide. J Sep Sci. 2010;33:1604-9.
- Aravind PR, Shajesh P, Mukundan P, Warrier KGK. Silica-titania aerogel monoliths with large pore volume and surface area by ambient pressure drying. J Sol-Gel Sci Technol. 2009;52:328-34.
- [41] Liu J-X, Shi F, Bai L-N, Feng X, Wang X-K, Bao L. Synthesis of TiO2-SiO2 aerogel via ambient pressure drying: effects of sol pre-modification on the microstructure and pore characteristics. J Sol-Gel Sci Technol. 2013;69:93-101.
- [42] Yang H, Zhu W, Sun S, Guo X. Preparation of monolithic titania aerogels with high surface area by a sol-gel process combined surface modification. RSC Adv. 2014;4:32934-40.
- Zhu J, Xie J, Lü X, Jiang D. Synthesis and characterization of superhydrophobic silica and silica/titania aerogels by sol-gel method at ambient pressure. Colloid Surface A. 2009;342:97-101.
- Kong Y, Shen X-D, Cui S. Direct synthesis of anatase TiO₂ aerogel resistant to high temperature under supercritical ethanol. Mater Lett. 2014;117:192-4.
- Sui R, Rizkalla A, Charpentier PA. Experimental study on the morphology and porosity of TiO2 aerogels synthesized in supercritical carbon dioxide. Micropor Mesopor Mat. 2011;142:688-95.
- [46] Paris C, Karelovic A, Manrique R, Le Bras S, Devred F, Vykoukal V, et al. CO2 hydrogenation to methanol with Gaand Zn-doped mesoporous Cu/SiO₂ catalysts prepared by the aerosol-assisted sol-gel Process. ChemSusChem. 2020;13:6409-17.
- Zhao L, Wang S, Wang Y, Li Z. Thermal stability of anatase TiO₂ aerogels. Surf Interface Anal. 2017;49:173-6.
- Bourikas K, Kordulis C, Lycourghiotis A. Titanium dioxide (anatase and rutile): Surface chemistry, liquid-solid interface chemistry, and scientific synthesis of supported catalysts. Chem Rev. 2014;114:9754-823.
- Diebold U. The surface science of titanium dioxide. Surf Sci [49] Rep. 2003;48:53-229.
- Ferreira-Neto EP, Ullah S, Perissinotto AP, de Vicente FS, Ribeiro SJL, Worsley MA, et al. Prussian blue as a co-catalyst for enhanced Cr(vi) photocatalytic reduction promoted by titania-based nanoparticles and aerogels. New J Chem. 2021;45:10217-31.

- [51] Locs J, Narkevica I, Bugovecka L, Ozolins J, Berzina-Cimdina L. Apatite-forming ability of thermally treated titania with various phase compositions. Mater Lett. 2015;146:69-72.
- [52] Amano F, Nakata M. High-temperature calcination and hydrogen reduction of rutile TiO2: A method to improve the photocatalytic activity for water oxidation. Appl Catal B. 2014;158-159:202-8.
- [53] O'Hayre R, Nanu M, Schoonman J, Goossens A. Mott-schottky and charge-transport analysis of nanoporous titanium dioxide films in air. J Phys Chem C. 2007;111:4809-14.
- [54] Lee HS, Woo CS, Youn BK, Kim SY, Oh ST, Sung YE, et al. Bandgap modulation of TiO2 and its effect on the activity in photocatalytic oxidation of 2-isopropyl-6-methyl-4-pyrimidinol. Top Catal. 2005;35:255-60.
- Zhao Z, Jiao X, Chen D. Preparation of ${\rm TiO_2}$ aerogels by a [55] sol-gel combined solvothermal route. J Mater Chem. 2009;19:3078.
- [56] Choi H, Carboni M, Kim YK, Jung CH, Moon SY, Koebel MM, et al. Synthesis of high surface area TiO2 aerogel support with Pt nanoparticle catalyst and CO oxidation study. Catal Lett. 2018;148:1504-13.
- Pap Z, Radu A, Hidi IJ, Melinte G, Diamandescu L, Popescu T, [57] et al. Behavior of gold nanoparticles in a titania aerogel matrix: Photocatalytic activity assessment and structure investigations. Chinese J Catal. 2013;34:734-40.
- [58] Li X, Wang H, Chen J, Zhou Q, Xiao Z. An efficient electron storage photovoltaic cell based on TiO2/carbon aerogel composite prepared by in-situ method. Electrochim Acta. 2014;145:281-5.
- [59] Chen X, Ye X, He J, Pan L, Xu S, Xiong C. Preparation of Fe³⁺doped TiO2 aerogels for photocatalytic reduction of CO2 to methanol. J Sol-Gel Sci Technol. 2020;95:353-9.
- [60] Bernardes JC, Latocheski E, Müller D, Serpa RB, Domingos JB, Rambo CR. Multiphase TiO₂ aerogels incorporated with Pd for mixed catalysis in wide UV-Vis spectrum. Appl Nanosci. 2020;11:455-65.
- Gannoun C, Delaigle R, Eloy P, Debecker DP, Ghorbel A, [61] Gaigneaux EM. Sol-gel derived V₂O₅-TiO₂ mesoporous materials as catalysts for the total oxidation of chlorobenzene. Catal Commun. 2011:15:1-5.
- Giwa A, Jung SM, Kong J, Hasan SW. Combined process of [62] electrically-membrane bioreactor and TiO2 aerogel filtration for efficient wastewater treatment. J Water. Process Eng. 2019;28:107-14.
- [63] Hayashi T, Nakamura K, Suzuki T, Saito N, Murakami Y. OH radical formation by the photocatalytic reduction reactions of H₂O₂ on the surface of plasmonic excited Au-TiO2 photocatalysts. Chem Phys Lett. 2020;739:136958.
- [64] Luo L, Cooper AT, Fan M. Preparation and application of nanoglued binary titania-silica aerogel. J Hazard Mater. 2009;161:175-82.
- Shi M, Wei W, Jiang Z, Han H, Gao J, Xie J. Biomass-derived [65] multifunctional ${\rm TiO_2}/{\rm carbonaceous}$ aerogel composite as a highly efficient photocatalyst. RSC Adv. 2016;6:25255-66.
- [66] Kistler SS. Coherent expanded aerogels and jellies. Nature.
- [67] Karamikamkar S, Naguib HE, Park CB. Advances in precursor system for silica-based aerogel production toward improved mechanical properties, customized morphology, and

- multifunctionality: A review. Adv Colloid Interface Sci. 2020;276:102101.
- [68] Gurav JL, Jung I-K, Park H-H, Kang ES, Nadargi DY. Silica aerogel: synthesis and applications. J Nanomater. 2010;2010:1–11.
- [69] Zhang S, Zhang Z, Pei J, Li R, Zhang J, Cai J, et al. A novel TiO₂-SiO₂ aerogel nanocomposite absorbent: preparation, characterization and photocatalytic degradation effects on automobile exhaust. Mater Res Express. 2018;5:025036.
- [70] Guangwu L, Yangang L. Preparation and characterization of silica-titania aerogel monoliths by sol-gel method. Proceedings of the 16th International Conference on Nanotechnology; 2016.
- [71] Brown LB, Anderson AM, Carroll MK. Fabrication of titania and titania-silica aerogels using rapid supercritical extraction. J Sol-Gel Sci Technol. 2012;62:404-13.
- [72] Shi F, Liu JX, Tang NL, Dong XL, Zhang XX, Bai LN, et al. Preparation of SiO₂ aerogel supported nano-TiO₂ photocatalysts for removing rhodamine B in the waste water. Adv Mat Res. 2012;531:494–8.
- [73] Zu G, Shen J, Wang W, Zou L, Lian Y, Zhang Z. Silica-titania composite aerogel photocatalysts by chemical liquid deposition of titania onto nanoporous silica scaffolds. ACS Appl Mater Inter. 2015;7:5400-9.
- [74] Wang H-L, Liang W-Z, Jiang W-F. Solar photocatalytic degradation of 2-sec-butyl-4,6-dinitrophenol (DNBP) using TiO₂/SiO₂ aerogel composite photocatalysts. Mater Chem Phys. 2011;130:1372-9.
- [75] Kim YN, Shao GN, Jeon SJ, Imran SM, Sarawade PB, Kim HT. Sol-gel synthesis of sodium silicate and titanium oxychloride based TiO₂-SiO₂ aerogels and their photocatalytic property under UV irradiation. Chem Eng J. 2013;231:502-11.
- [76] Yao N, Cao S, Yeung KL. Mesoporous TiO₂-SiO₂ aerogels with hierarchal pore structures. Micropor Mesopor Mat. 2009;117:570-9.
- [77] Lee KY, Park SM, Kim JB, El Saliby I, Shahid M, Kim GJ, et al. Synthesis and characterisation of porous titania-silica composite aerogel for NO_x and acetaldehyde removal. J Nanosci Nanotechnol. 2016;16:4505–11.
- [78] Ingale SV, Wagh PB, Tripathi AK, Dudwadkar AS, Gamre SS, Rao PT, et al. Photo catalytic oxidation of TNT using TiO₂-SiO₂ nano-composite aerogel catalyst prepared using sol-gel process. J Sol-Gel Sci Technol. 2011;58:682-8.
- [79] Lázár I, Kalmár J, Peter A, Szilágyi A, Győri E, Ditrói T, et al. Photocatalytic performance of highly amorphous titania-silica aerogels with mesopores: The adverse effect of the in situ adsorption of some organic substrates during photodegradation. Appl Surf Sci. 2015;356:521-31.
- [80] Parale VG, Kim T, Lee K-Y, Phadtare VD, Dhavale RP, Jung H-N-R, et al. Hydrophobic TiO₂-SiO₂ composite aerogels synthesized via *in situ* epoxy-ring opening polymerization and sol-gel process for enhanced degradation activity. Ceram Int. 2020;46:4939-46.
- [81] Beauger C, Testut L, Berthon-Fabry S, Georgi F, Guetaz L. Doped TiO₂ aerogels as alternative catalyst supports for proton exchange membrane fuel cells: A comparative study of Nb, V and Ta dopants. Micropor Mesopor Mat. 2016;232:109–18.
- [82] Jiang N, Du Y, Lv X, Yang K, Du M, Feng Y, et al. Preparation and characterization of bifunctional Zn doped TiO₂ aerogels

- toward Rhodamine B in water. Mater Res Express. 2018:5:115511.
- [83] Popa M, Diamandescu L, Vasiliu F, Teodorescu CM, Cosoveanu V, Baia M, et al. Synthesis, structural characterization, and photocatalytic properties of iron-doped TiO₂ aerogels. J Mater Sci. 2009;44:358-64.
- [84] Rodriguez TR, Vargas S, Arroyo MR, MontielCR, Haro PE. Modification of the phase transition temperatures in titania doped with various cations. J Mater Res. 1997;12:439-43.
- [85] Guidi V, Carotta M, Ferroni M, Martinelli G, Sacerdoti M. Effect of dopants on grain coalescence and oxygen mobility in nanostructured titania anatase and rutile. J Phys Chem B. 2003;107:120-4.
- [86] Duan L, Jiang N, Lu N, Shang K, Li J, Wu Y. Synergetic effect of TiO_2 and Fe^{3+} as co-catalysts for enhanced phenol degradation in pulsed discharge system. Appl Catal B. 2018;221:521–9.
- [87] Wang NN, Yu CL, Dai HY, Fu YH, Shao GL, Dong XL. Ionic liquid-assisted synthesis of anatase nanostructured TiO₂ aerogel doped with Fe³⁺ by a low temperature sol-gel process and its photocatalytic performance. Adv Mat Res. 2013;785-786:365-9.
- [88] Reszczyńska J, Grzyb T, Sobczak JW, Lisowski W, Gazda M, Ohtani B, et al. Lanthanide co-doped TiO₂: The effect of metal type and amount on surface properties and photocatalytic activity. Appl Surf Sci. 2014;307:333-45.
- [89] Kibombo HS, Weber AS, Wu C-M, Raghupathi KR, Koodali RT. Effectively dispersed europium oxide dopants in TiO₂ aerogel supports for enhanced photocatalytic pollutant degradation. J Photoch Photobio A. 2013;269:49–58.
- [90] Lin Z, Wang X, Liu J, Tian Z, Dai L, He B, et al. On the role of localized surface plasmon resonance in UV-Vis light irradiated Au/TiO₂ photocatalysis systems: pros and cons. Nanoscale. 2015;7:4114-23.
- [91] Zhang T, Xu M, Li J. Enhanced photocatalysis of TiO₂ by aluminum plasmonic. Catal Today. 2021;376:162-7.
- [92] Dahlman CJ, Agrawal A, Staller CM, Adair J, Milliron DJ.

 Anisotropic origins of localized surface plasmon resonance in n-Type anatase TiO₂ nanocrystals. Chem Mater.

 2019:31:502–11.
- [93] Cushing SK, Li J, Bright J, Yost BT, Zheng P, Bristow AD, et al. Controlling plasmon-induced resonance energy transfer and hot electron injection processes in metal@TiO₂ core-shell nanoparticles. J Phys Chem C. 2015;119:16239-44.
- [94] DuChene JS, Williams BP, Johnston-Peck AC, Qiu J, Gomes M, Amilhau M, et al. Elucidating the sole contribution from electromagnetic near-fields in plasmon-enhanced Cu_2O photocathodes. Adv Energy Mater. 2016;6:1501250.
- [95] Jing F, Suo H, Cui S, Tang X, Zhang M, Shen X, et al. Facile synthesis of TiO₂/Ag composite aerogel with excellent antibacterial properties. J Sol-Gel Sci Technol. 2018;86:590-8.
- [96] Pennington AM, Pitman CL, DeSario PA, Brintlinger TH, Jeon S, Balow RB, et al. Photocatalytic CO oxidation over nanoparticulate Au-modified TiO₂ aerogels: The importance of size and intimacy. ACS Catal. 2020;10:14834–46.
- [97] DeSario PA, Gordon WO, Balboa A, Pennington AM, Pitman CL, McEntee M, et al. Photoenhanced degradation of sarin at Cu/TiO₂ composite aerogels: roles of bandgap excitation and surface plasmon excitation. ACS Appl Mater Inter. 2021;13:12550-61.

- [98] DeSario PA, Pitman CL, Delia DJ, Driscoll DM, Maynes AJ, Morris JR, et al. Low-temperature CO oxidation at persistent low-valent Cu nanoparticles on ${\rm TiO_2}$ aerogels. Appl Catal B. 2019;252:205-13.
- [99] Hu L, Wang R, Wang M, Wang C, Xu Y, Wang Y, et al. The inactivation effects and mechanisms of Karenia mikimotoi by non-metallic elements modified TiO₂ (SNP-TiO₂) under visible light. Sci Total Environ. 2022;820:153346.
- [100] Somekawa S, Kusumoto Y, Ikeda M, Ahmmad B, Horie Y. Fabrication of N-doped TiO₂ thin films by laser ablation method: Mechanism of N-doping and evaluation of the thin films. Catal Commun. 2008;9:437-40.
- Popa M, Macovei D, Indrea E, Mercioniu I, Popescu IC, Danciu V. Synthesis and structural characteristics of nitrogen doped TiO2 aerogels. Micropor Mesopor Mat. 2010;132:80-6.
- [102] Parale VG, Kim T, Phadtare VD, Yadav HM, Park H-H. Enhanced photocatalytic activity of a mesoporous TiO₂ aerogel decorated onto three-dimensional carbon foam. J Mol Liq. 2019;277:424-33.
- [103] Wang H, Liu H, Wang S, Li L, Liu X. Influence of tunable pore size on photocatalytic and photoelectrochemical performances of hierarchical porous TiO₂/C nanocomposites synthesized via dual-templating. Appl Catal B. 2018;224:341-9.
- [104] Zhou Y, Yi Q, Xing M, Shang L, Zhang T, Zhang J. Graphene modified mesoporous titania single crystals with controlled and selective photoredox surfaces. Chem Commun. 2016;52:1689-92.
- [105] Sun X, Ji S, Wang M, Dou J, Yang Z, Qiu H, et al. Fabrication of porous TiO2-RGO hybrid aerogel for high-efficiency, visiblelight photodegradation of dyes. J Alloys Compd. 2020;819:153033.
- [106] Zheng T, Li A, Li Z, Hu W, Shao L, Lu L, et al. Mechanical reinforcement of a cellulose aerogel with nanocrystalline cellulose as reinforcer. RSC Adv. 2017;7:34461-5.
- [107] Liu Z, Wu P, Yang S, Wang H, Jin C. Synthesis and characterization of uniform spherical nanoporous TiO2 aerogel templated by cellulose alcohol-gel with enhanced photocatalytic activity. Int J Polym Sci. 2016;2016:1-8.
- [108] Lu Y, Sun QF, Li J, Liu YX. Fabrication, characterization and photocatalytic activity of TiO2/cellulose composite aerogel. Key Eng Mater. 2014;609-610:542-6.
- [109] Ho DP, Vigneswaran S, Ngo HH. Integration of photocatalysis and microfiltration in removing effluent organic matter from treated sewage effluent. Sep Sci Technol. 2010;45:155-62.
- [110] Yang H, Jiang L, Li Y, Li G, Yang Y, He J, et al. Highly efficient red cabbage anthocyanin inserted TiO2 aerogel nanocomposites for photocatalytic reduction of Cr(VI) under Visible Light. Nanomaterials. 2018;8:937.
- Li Y, Yang Y, Yang P, Jiang L, Wang W, He J, et al. Tungstate doped TiO2-SiO2 aerogels for preferential photocatalytic degradation of methamphetamine in seizure samples containing caffeine under simulated sunlight. Catal Commun. 2020;145:106121.
- [112] Moon S-C, Mametsuka H, Tabata S, Suzuki E. Photocatalytic production of hydrogen from water using TiO₂ and B/TiO₂. Catal Today. 2000;58:125-32.
- Jeong S, Chung K-H, Lee H, Park H, Jeon K-J, Park Y-K, et al. Effect of liquid phase plasma on photocatalysis of water

- for hydrogen evolution. Int J Hydrogen Energy. 2017:42:17386-93.
- [114] Qin Z, Chen L, Ma R, Tomovska R, Luo X, Xie X, et al. TiO₂/BiYO₃ composites for enhanced photocatalytic hydrogen production. J Alloys Compd. 2020;836:155428.
- Indrea E, Dreve S, Silipas TD, Mihailescu G, Danciu V, Cosoveanu V, et al. Nanocrystalline semiconductor materials for solar water-splitting. J Alloys Compd. 2009;483:445-9.
- [116] Chang L, Sun Z, Hu YH. 1T phase transition metal dichalcogenides for hydrogen evolution reaction. Electrochem Energy Rev. 2021;4:194-218.
- Wu H, Feng C, Zhang L, Zhang J, Wilkinson DP. Non-noble metal electrocatalysts for the hydrogen evolution reaction in water electrolysis. Electrochem Energy Rev. 2021;4:473-507.
- [118] Liao C-H, Huang C-W, Wu JCS. Hydrogen production from semiconductor-based photocatalysis via water splitting. Catalysts. 2012;2:490-516.
- [119] Bell S, Will G, Bell J. Light intensity effects on photocatalytic water splitting with a titania catalyst. Int J Hydrogen Energy. 2013:38:6938-47.
- [120] Puskelova J, Baia L, Vulpoi A, Baia M, Antoniadou M, Dracopoulos V, et al. Photocatalytic hydrogen production using TiO₂-Pt aerogels. Chem Eng J. 2014;242:96-101.
- [121] Lin C-C, Wei T-Y, Lee K-T. Lu S-Y. Titania and Pt/titania aerogels as superior mesoporous structures for photocatalytic water splitting. J Mater Chem. 2011;21:12668.
- [122] Zheng X-J, Wei L-F, Zhang Z-H, Jiang Q-J, Wei Y-J, Xie B, et al. Research on photocatalytic H2 production from acetic acid solution by Pt/TiO₂ nanoparticles under UV irradiation. Int J Hydrogen Energy. 2009;34:9033-41.
- Tan H, Zhao Z, Niu M, Mao C, Cao D, Cheng D, et al. A facile and versatile method for preparation of colored TiO2 with enhanced solar-driven photocatalytic activity. Nanoscale. 2014;6:10216-23.
- [124] Yoo SJ, Lee K-S, Cho Y-H, Kim S-K, Lim T-H, Sung Y-E. Electrocatalytic properties of TiO₂-embedded Pt nanoparticles in oxidation of methanol: Particle size effect and proton spillover effect. Electrocatalysis. 2011;2:297-306.
- [125] Xing J, Li YH, Jiang HB, Wang Y, Yang HG. The size and valence state effect of Pt on photocatalytic H2 evolution over platinized TiO2 photocatalyst. Int J Hydrogen Energy. 2014;39:1237-42.
- [126] Fort CI, Pap Z, Indrea E, Baia L, Danciu V, Popa M. Pt/N-TiO₂ aerogel composites used for hydrogen production via photocatalysis process. Catal Lett. 2014;144:1955-61.
- DeSario PA, Pietron JJ, DeVantier DE, Brintlinger TH, [127] Stroud RM, Rolison DR. Plasmonic enhancement of visiblelight water splitting with Au-TiO₂ composite aerogels. Nanoscale. 2013;5:8073-83.
- [128] Kim S, Cho Y, Rhee R, Park JH. Black TiO2: What are exact functions of disorder layer. Carbon. Energy. 2020:2:44-53.
- [129] Xue X, Qiu M, Li Y, Zhang QM, Li S, Yang Z, et al. Creating an eco-friendly building coating with smart subambient radiative cooling. Adv Mater. 2020;e1906751.
- [130] Su L, Wang H, Niu M, Dai S, Cai Z, Yang B, et al. Anisotropic and hierarchical SiC@SiO2 nanowire aerogel with exceptional stiffness and stability for thermal superinsulation. Sci Adv. 2020;6:eaay6689.

- [131] Xu X, Zhang Q, Hao M, Hu Y, Lin Z, Peng L, et al. Doublenegative-index ceramic aerogels for thermal superinsulation. Science. 2019;363:723-7.
- [132] Zu G, Shena J, Wanga W, Liana Y, Zoua L, Zhangb Y, et al. Heat-resistant, strong titania aerogels achieved by supercritical deposition. J Supercrit Fluids. 2015;106:145-51.
- [133] Si Y, Wang X, Dou L, Yu J, Ding B. Ultralight and fire-resistant ceramic nanofibrous aerogels with temperature-invariant superelasticity. Sci Adv. 2018;4:eaas8925.
- [134] Zhao S, Malfait WJ, Jeong E, Fischer B, Zhang Y, Xu H, et al. Facile one-pot synthesis of mechanically robust biopoly-
- mer-silica nanocomposite aerogel by cogelation of silicic acid with chitosan in aqueous media. ACS Sustain. Chem Eng. 2016;4:5674-83.
- [135] Roth TB, Anderson AM, Carroll MK. Analysis of a rapid supercritical extraction aerogel fabrication process: Prediction of thermodynamic conditions during processing. J Non-Cryst Solids. 2008;354:3685–93.
- [136] Anderson AM, Wattley CW, Carroll MK. Silica aerogels prepared via rapid supercritical extraction: Effect of process variables on aerogel properties. J Non-Cryst Solids. 2009;355:101–8.